Study of High Energy Electron Cooling (2 MeV) and Stochastic Cooling with Different Internal Targets

Final report

I.N.Meshkov, A.O. Sidorin, A.V.Smirnov
Joint Institute for Nuclear Research, Dubna, Russia

CONTENTS

INTRODUCTION

Necessity of the high energy electron cooling at COSY is determined by the beginning of experiments at the WASA target [1]. The goal of the cooling system is to provide maximum average luminosity and maximum luminosity life-time. The cooling system design was performed in [2].

At small energy and/or high target density the dominating process in beam-target interaction is ionization energy losses. At the required range of the target density and beam energy this effect can not be compensating either by stochastic or electron cooling. If the ionization energy losses are compensated by RF the main heating effects will be emittance growth due to multiple scattering in the target and momentum spread growth due to fluctuations of the energy losses. The emittance growth rate can be decreased by a choice of appropriate small beta-function value in the target position. In this case the general heating effects can be suppressed by a cooling.

The problem of energy loss compensation is common for all experiments with internal target. For instance at HESR to compensate the energy loss in PANDA experiment one plan to use a barrier-bucket system. In this case the required small momentum spread is obtained by the common action of stochastic and electron cooling system. At COSY energy the problem of the ionization energy loss is more crucial due to smaller beam energy. (The target density in both cases is practically the same).

The beam intensity required to reach the maximum WASA luminosity is about $5 \cdot 10^{10}$ particles, that lies in the range of effective stochastic cooling application. However, the existing COSY stochastic cooling system can not be operated with a bunched beam. Therefore the problem of the beam cooling at high target density can be solved by two ways:

- implementation of a barrier-bucket system and application of the stochastic cooling system (if the existing stochastic cooling can work together with a barrier-bucket),
- electron cooling of the bunched beam.

A few experiments are planned to be provided at minimum proton momentum of 2.25 GeV/c, when the stochastic cooling efficiency is pure due to small momentum slip factor value. The beam cooling at this energy can be provided by electron cooling system.

In the first chapter of this report general effects acting on the beam quality in interaction with internal targets and peculiarity of WASA pellet target are described.

In the second chapter results of numerical simulations of electron cooling application in experiment with a pellet target are presented. Comparison between magnetized and non-magnetized cooling is done.

In the third chapter application of existing stochastic cooling system is analyzed when the ionization energy loss is compensated by RF.

Friction force formulae used for electron cooling simulations and the pellet target model are described in the Addendum.

1. LUMINOSITY OF EXPERIMENT WITH INTERNAL TARGET

1.1. Uniform target

Peak luminosity in the case of beam interaction with a uniform internal target at thickness of ρ [Atoms/cm^2] is given by

$$L = \frac{N\rho}{T_{rev}} \tag{1.1}$$

where N is the number of ions circulating in the ring, T_{rev} is the revolution period. The average luminosity $\langle L \rangle$ is determined by the beam preparation time t_{prep} and experiment time (beam on target per experiment cycle) t_{exp} as

$$\langle L \rangle = \frac{\int_0^{t_{\exp}} L dt}{t_{\exp} + t_{prep}}. \tag{1.2}$$

The luminosity time dependence can be found from the equation

$$\frac{dL}{dt} = \frac{\rho}{T_{rev}} \frac{dN}{dt}, \tag{1.3}$$

where the ion number variation is caused by particle loss due to interaction with the target and other losses caused by interaction with residual gas atoms and, in the case of electron cooling application, by recombination in electron cooling section.

The particle loss in the target is proportional to the luminosity value

$$\frac{dN}{dt} = -L\sigma_{tot} \tag{1.4}$$

and determined by three general processes – electron capture by the ion, single Coulomb scattering on large angle and inelastic scattering with the target nuclei leading to the particle loss.

Interaction with the residual gas leads to the particle losses

$$\frac{dN}{dt} = -\frac{N}{T_{rev}} \rho_{gas} \sigma_{tot,gas} \tag{1.5}$$

where the cross-section depends on residual gas composition. The residual gas thickness can be estimated as

$$\rho_{gas[atoms/\mathrm{cm}^2]} = 3.6 \cdot 10^{16} P_{[Torr]} \cdot C_{[cm]} \tag{1.6}$$

where P is the average pressure in the ring, C is the ring circumference. At the residual gas pressure of 10^{-9} Torr the thickness is equal to about $7 \cdot 10^{12}$ Atoms/cm^2. Therefore, at internal target thickness over 10^{14} atoms/cm^2 the beam interaction with the residual gas is negligible.

In the case of electron cooling application the beam life time due to recombination in the cooling section depends on electron velocity spread, electron density and the cooling section length. At design parameters of COSY high energy electron cooling system (see Table 2.1 in the chapter 2) the loss rate due to recombination is presented in Table 1.1 together with the loss rates due to interaction with a hydrogen target of the thickness of $2 \cdot 10^{15}$ Atoms/cm^2. The loss rate due to single scattering on large angles was calculated for the acceptance values of 60 π·mm·mrad in the horizontal plane and 24 π·mm·mrad in the vertical one that corresponds to COSY acceptance at usual operational conditions. The total cross-section of *pp* collisions is almost constant in the experiment energy range and equal to about 40 mbarn.

Table.1.1. Particle loss rates at different proton momentum.

Proton momentum [GeV/c]	**2.25**	**3.7**
Electron capture in cooler (Ie = 0.2 A) [1/sec]	-2.4×10^{-7}	-9.2×10^{-8}
Electron capture in target [1/sec]	-7.6×10^{-17}	-3.5×10^{-18}
Single scattering on target atoms [1/sec]	-6.7×10^{-5}	-2.5×10^{-5}
pp collisions in target (σ = 40 mbarn) [1/sec]	-1.2×10^{-4}	-1.2×10^{-4}

The beam life-time is limited mainly by the interaction with the target. In this case the luminosity time dependence can be found analytically from the differential equation

$$\frac{dL}{dt} = -L\frac{\rho\sigma_{tot}}{T_{rev}}. \tag{1.7}$$

The average luminosity can be expressed as

$$\langle L \rangle = L_0 \frac{\tau\left(1-\exp(-t_{\exp}/\tau)\right)}{t_{\exp}+t_{prep}}, \tag{1.8}$$

where the luminosity life-time

$$\tau = \frac{T_{rev}}{\rho\sigma_{tot}} \tag{1.9}$$

is determined mainly by inelastic collision and at target density of $2 \cdot 10^{15}$ Atoms/cm^2 the life time is about 2 hours. The beam preparation time can be estimated as 10 – 20 sec [3] and if all the heating effects are suppressed by stochastic or electron cooling the experiment time can be chosen to be

$$\tau >> t_{exp} >> t_{prep},$$

and experiment will be performed at almost constant luminosity.

1.2. Limitations of the experiment time

Without cooling the experiment time is limited by the beam heating during interaction with a target. General effects leading to increase of six dimensional phase volume and change of mean energy are:

- mean (ionization) energy loss;
- fluctuations of the energy loss leading to increase of the beam momentum spread;
- multiple scattering on the target atoms leading to emittance growth.

1.2.1. Mean energy losses

Mean energy loss in the target can be calculated in accordance with the Bethe-Bloch equation:

$$\frac{\Delta E}{\rho} = -KZ_P^2 \frac{Z_T}{A_T} \frac{1}{\beta^2} \left[\frac{1}{2} \ln \frac{2m_e c^2 \beta^2 \gamma^2 E_{\max}}{I^2} - \beta^2 - \frac{\delta}{2} \right] \tag{1.10}$$

ρ – target density in g/cm^2, Z_P and Z_T are the charge number of projectile and target atoms, A_T is the target atomic number. K is a constant determining by the following expression:

$$\frac{K}{A} = \frac{4\pi N_A r_e^2 m_e c^2}{A} = 0.307075 \text{ MeV}\cdot\text{g}^{-1}\cdot\text{cm}^2, \tag{1.11}$$

r_e is the electron classic radius, N_A is Avogadro number. $E_{\max}$ is the maximum transferable energy:

$$E_{\max} = \frac{2m_e c^2 \beta^2 \gamma^2}{1 + 2\gamma \frac{m_e}{M} + \left(\frac{m_e}{M} \right)^2}$$

with m_e is the electron mass and M - the projectile mass. I is the mean excitation energy, which is equal to 13.6 eV for hydrogen and (10±1)·Z eV for elements heavier than sulphur.

The density effect correction factor $\delta/2$ in the equation (1.10) is much larger for a liquid or solid than for a gas and at very high energies

$$\frac{\delta}{2} \to \ln \frac{\hbar\omega_p}{I} + \ln \beta\gamma - \frac{1}{2}, \tag{1.12}$$

where the plasma energy $\hbar\omega_p$ is determined by electron density in the target:

$$\hbar\omega_p = \sqrt{4\pi n_e r_e^3}\, m_e c^2 / \alpha = 28.816 \sqrt{\rho_{[g/cm^3]} \left\langle \frac{Z}{A} \right\rangle} [eV] \tag{1.13}$$

Here α is the fine structure constant.

In the calculations presented here the equation (1.10) is simplified in accordance with [4] by introducing of the quantity ξ, which is proportional to the thickness ρ of the target in [g/cm^2]:

$$\xi = 0.1535 \left[\frac{MeV\, cm^2}{g} \right] \frac{Z_P^2}{\beta^2} \frac{Z_T}{A_T} \rho \,. \tag{1.14}$$

Neglecting the effect density correction one can express the mean energy loss in the following form:

$$\Delta E = 2\xi \left(\ln \frac{E_{\max}}{I} - \beta^2 \right). \tag{1.15}$$

The mean energy loss is main effect limiting the experiment time. In the Fig. 1.1 one can see that when the momentum deviation increases to about longitudinal acceptance value, the beam emittance increases by about 50% only and rms momentum spread increases by about two times. If the energy loss does not compensated, after about three minutes of the experiment the mean beam energy decreases to the acceptance limit that leads fast particle loss and decrease of luminosity.

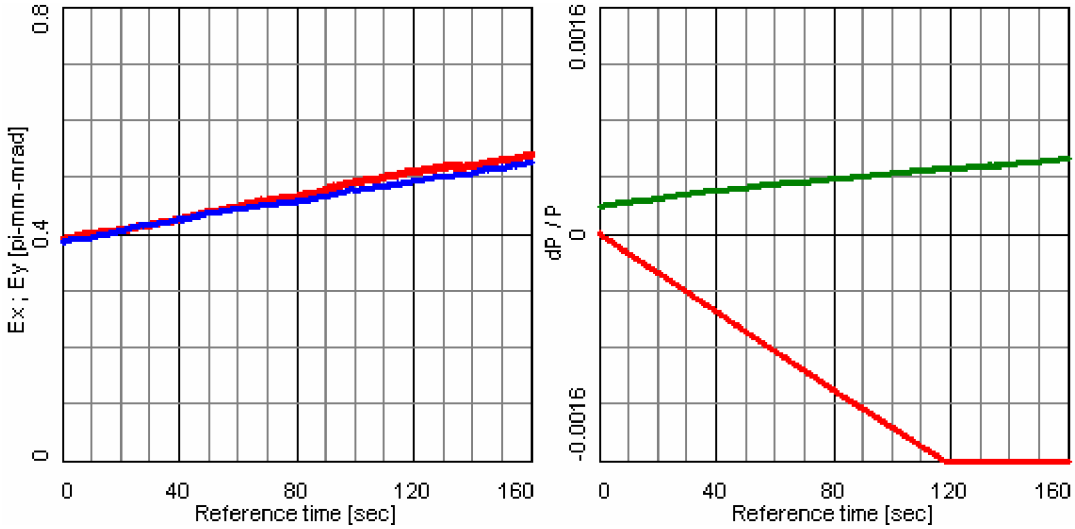

Fig.1.1. Emittance (left plot) and momentum spread (right plot) evolution in time due to interaction with internal target. The target density is $2 \cdot 10^{15}$ Atoms/cm^2. Grin line in the right plot is the relative momentum spread, red line – relative momentum deviation from its initial value.

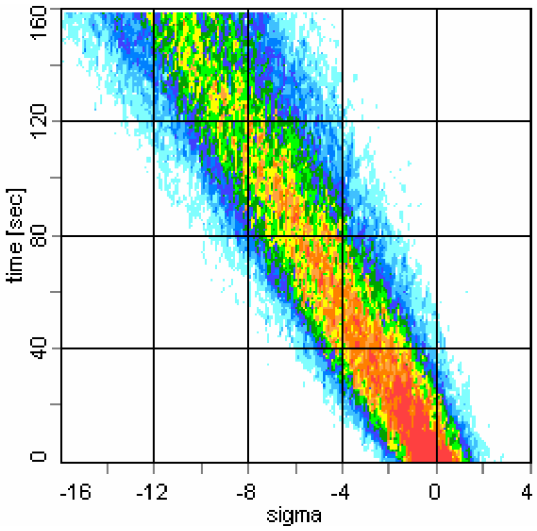

Fig. 1.2. Evolution of momentum spread distribution on time. The momentum is measured in initial rms width (sigma). The initial rms width is equal to $2 \cdot 10^{-4}$.

Electron cooling application can not suppress completely this process. Even at 3 A of electron current can stabilizes only the central part of distribution, but the low energy tail increases with time and leads to particle loss after a few minutes of experiment (Fig. 1.3, 1.4).

However the mean energy loss can be compensated by application of RF at relatively small amplitude, or by usage of Barrier bucket system. The bunching factor (peak to mean current ratio) has to be small enough to avoid increase of phase space growth due to intrabeam scattering.

When the mean energy losses are compensated by RF, the experiment time is limited by momentum spread and emittance growth leading to particle loss at corresponding acceptance.

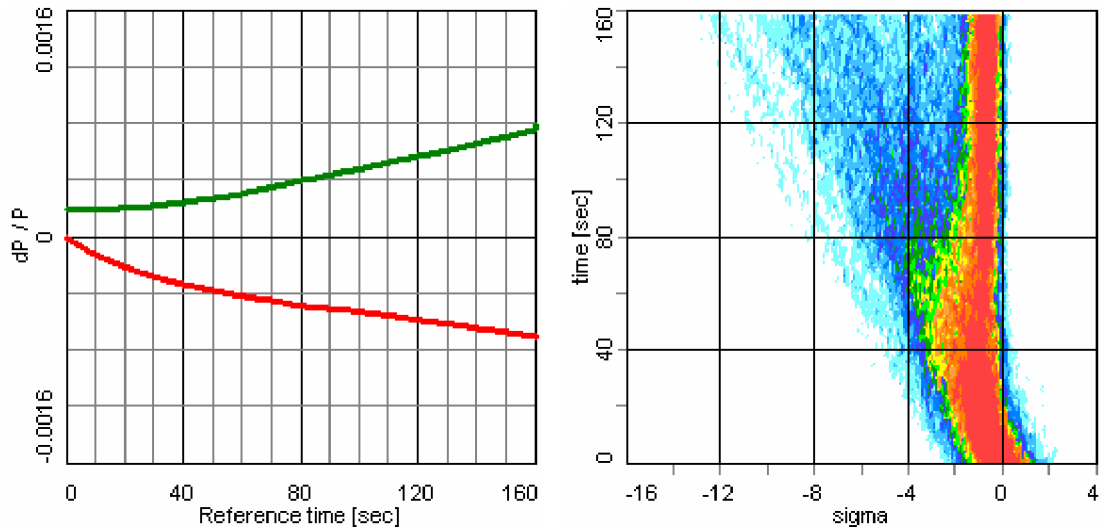

Fig.1.3. Momentum spread (grin line in the left plot), momentum deviation (red line in the left plot) and momentum spread evolution (right plot) on time during interaction with internal target and electron cooling. Initial rms momentum spread is equal to $2 \cdot 10^{-4}$, the target density is $2 \cdot 10^{15}$ Atoms/cm^2, electron beam current is 3 A.

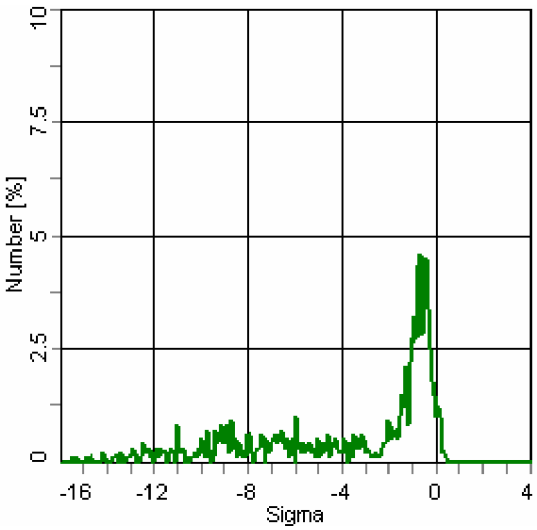

Fig. 1.4. Momentum spread distribution after 160 sec of interaction with internal target and electron cooling. Parameters are the same as in Fig. 1.3.

1.2.2. Energy loss fluctuations

The energy loss determined by (1.15) is the mean value. For finite target thickness there are fluctuations of the energy loss. The ion distribution is skewed toward high values (Landau tail). For a thick layer (when $\Delta E >> E_{max}$) the distribution is nearly Gaussian. The square of the standard deviation of the ion distribution function in the energy space for a thick target is given by:

$$E_{str}^2 = \xi E_{\max}\left(1-\frac{\beta^2}{2}\right), \qquad (1.16)$$

where ξ is given by the formula (1.14). The fluctuations of the energy loss lead to increase of the ion beam momentum spread after single crossing the target in accordance with:

$$\left(\Delta\sigma_p\right)^2_{str} = \left(\frac{\gamma}{\gamma+1}\right)^2 \frac{E^2_{str}}{E^2}. \tag{1.17}$$

This process causes a linear increase of square of the momentum spread in time:

$$\frac{d\sigma^2_p}{dt} = \frac{\left(\Delta\sigma_p\right)^2_{str}}{T_{rev}}, \tag{1.18}$$

and the derivative is scaled linearly with the target thickness (see 1.14). At the target thickness of $2\cdot10^{15}$ Atoms/cm^2 it equal to about

$$\frac{d\sigma^2_p}{dt} = 2.4\cdot10^{-10}\,\frac{rad^2}{s},$$

and this process does not limit practically the experiment time.

1.2.3. Emittance growth

In absence of dispersion in the target position the emittance of the beam increases linearly with time. The derivative is determined by rms value of the scattering angle due to multiple scattering on the target atoms:

$$\frac{d\varepsilon_{x,y}}{dt} = \frac{\beta_{x,y}\theta^2_{rms}}{2T_{rev}}. \tag{1.19}$$

Square of the rms scattering angle linearly scales with the target thickness:

$$\theta^2_{str} = 2\rho\pi\left(\frac{Z_T Z_P r_p}{A_P \beta^2 \gamma}\right)^2\left[\ln\left(\frac{\alpha_2^2}{\chi^2}\right) - 1 + \Delta b\right], \tag{1.20}$$

where r_p is the classical proton radius. The parameters α_2, χ and Δb are determined by properties of projectile and target nucleus and practically does not depend on energy.

The experiment time limited by this process can be estimated as

$$t_{\exp} \le \frac{2(A/6)}{\beta\theta^2_{rms}} T_{rev}, \tag{1.21}$$

where A is the ring acceptance. At the target thickness of $2\cdot10^{15}$ Atoms/cm^2 the estimation (1.21) gives about 10^4 sec (at beta function equal to 3 m and vertical acceptance of 24 π·mm·mrad). Thus, if the mean energy loss is compensated, the experiment time is limited by particle loss due to inelastic scattering in the target and can be about 1 hour. At minimum experiment energy the emittance growth can limit the experiment time due to strong enough dependence of the rms scattering angle on energy. It should be noted that this conclusion relates to uniform target only. The limitations of the experiment time at interaction with a pellet target are described in the next paragraph.

1.3. Pellet target

A pellet flux has a finite radius which is sufficiently less then the vacuum chamber aperture. Therefore if an amplitude of the particle betatron oscillations becomes to be larger than the flux radius due to emittance growth the probability of the target crossing decreases. Thus the emittance growth due to multiple scattering on the target atoms leads to additional decrease of the luminosity. This effect can be roughly estimated by introducing into (1.1) an effective thickness instead of real one. The target effective thickness can be estimated as averaging of real thickness over the ion distribution:

$$\rho_{eff} = \int \rho(x) f(x) dx, \tag{1.22}$$

where $f(x)$ is the ion distribution over the horizontal co-ordinate. The dependence of the flux thickness on horizontal co-ordinate in the case of cylindrical flux and uniform distribution of the pellets inside it can be written as:

$$\rho(x) = \langle \Re \rangle \begin{cases} 2\sqrt{r_f^2 - x^2} & if \quad |x| < r_f \\ 0 \quad if & |x| \geq r_f \end{cases} \tag{1.23}$$

where r_f is the pellet flux radius. $\langle \Re \rangle$ is the mean target density in Atoms/cm^3 which can be estimated as

$$\langle \Re \rangle = \frac{\frac{4}{3}\pi r_p^3}{\pi r_f^2 \langle h \rangle} \Re \tag{1.24}$$

where $\Re$ = 4.3·10^{21} Atoms/cm^3 is the frozen hydrogen density, $\langle h \rangle$ is the mean distance between pellets in the vertical direction. The pellet target geometry corresponding to this model is sketched in the Fig. 1.5. More accurate model of the pellet target is described in the Appendix to this report.

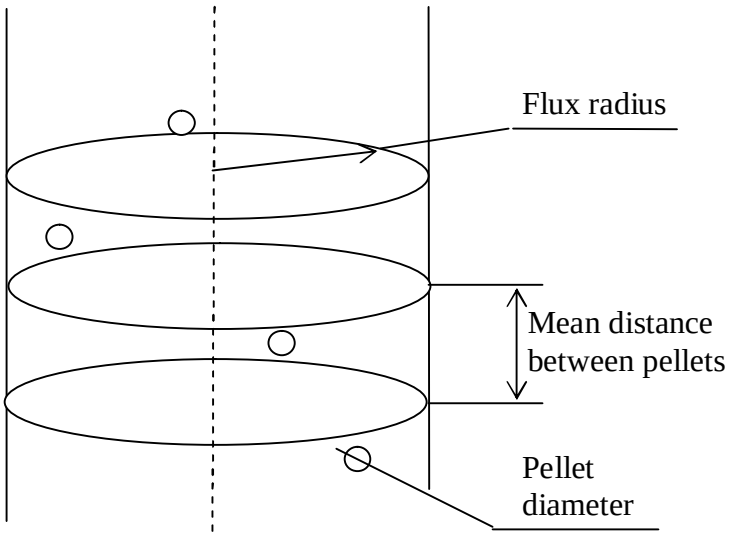

Fig. 1.5. Schematics of the pellet target geometry. The pellets move in the vertical direction from top to bottom with equal velocities.

Assuming Gaussian distribution of the ions

$$f(x) = \frac{1}{\sqrt{2\pi}\sigma_x} e^{-\frac{x^2}{2\sigma_x^2}} \tag{1.25}$$

one can calculate the effective target thickness as function of the beam rms size in the target position (Fig. 1.6). The pellet target parameters are taken from the Table 2.1 in the next chapter.

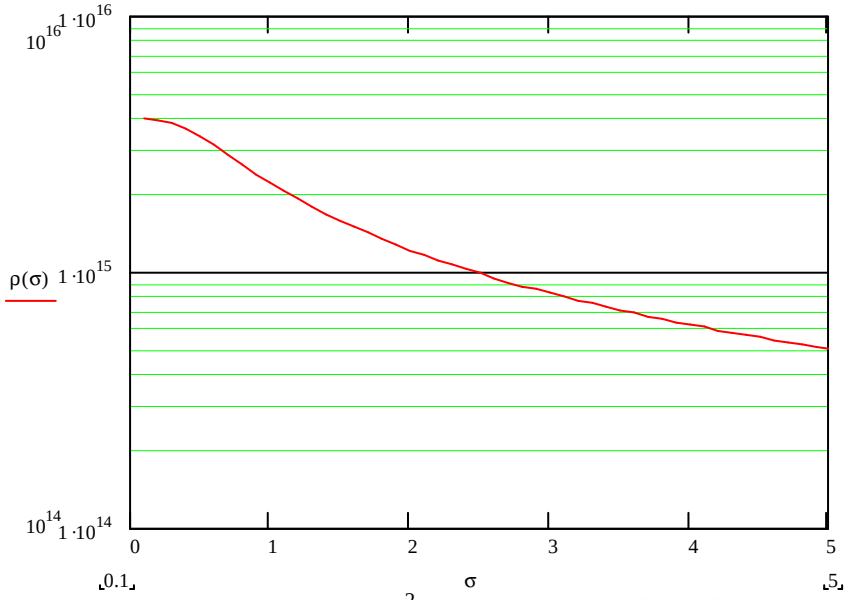

Fig. 1.6. Effective target thickness in Atoms/cm^2 versus horizontal rms beam size in mm. The flux radius is 1 mm. The target parameters are listed in the Table 2.1.

At the beta function in the target position of 3 m the beam size of 5 mm corresponds to emittance equal $A_x/6$, where A_x is the ring horizontal acceptance (from this value one can expect the particle loss on aperture). When the beam emittance increases from 0.4 π·mm·mrad (beam size is equal to pellet flux radius) to this value the luminosity decreases by about 5 times, in difference with uniform target where the luminosity is constant.

For optimum choice of the beam emittance in experiment with the pellet target one can investigate the effective target thickness calculated for a particle at some amplitude of horizontal betatron oscillations A:

$$\rho_{single} = \frac{1}{2\pi}\int_0^{2\pi} \rho(A\cos\varphi)d\varphi \,. \tag{1.26}$$

This dependence shows that a fast decrease of the effective thickness begins when the amplitude of oscillations exceeds the flux radius (Fig. 1.7). To avoid sufficiently different heating rates for the particles in the beam core and in the tails the maximum amplitude of the oscillations can be chosen below 2 – 3 mm. The corresponding rms emittance lies between 0.1 and 0.4 π·mm·mrad. In the numerical simulations presented in this report the initial emittance is chosen to be 0.4 π·mm·mrad in both transverse planes.

Assuming that at injection the COSY acceptance is filled uniformly, the horizontal beam emittance after acceleration can be estimated by the value of about 6 π·mm·mrad therefore a precooling of the

beam is necessary. Before beginning of the experiment the initial emittance has to be decreased by about 20 times. It can be done using electron cooling at injection energy or stochastic/electron cooling at energy of experiment. The precooling time has to be taken into account in the beam preparation time calculation. Electron cooling at injection energy requires about 10 sec, stochastic cooling at energy of experiment – about 2 minutes.

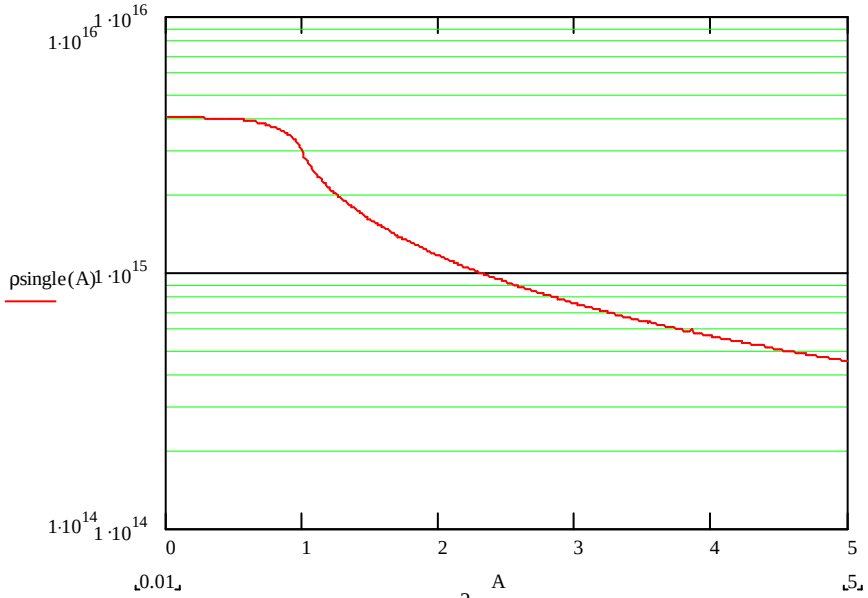

Fig. 1.7. Effective target thickness in Atoms/cm^2 versus amplitude of the particle horizontal betatron oscillations in mm. The flux radius is 1 mm. The target parameters are listed in the Table 2.1.

If the beam emittance is stable during experiment the pellet target can be treated as an uniform target at corresponding effective thickness. Granularity and finite dimensions of the target can lead to inclination of the distribution function from Gaussian shape (in the horizontal plane mainly) that is not so important for the experiment.

Suppression of the emittance growth by a cooling permits to provide experiment during long period of time at almost constant luminosity. To take into account all general effects acting on the beam distribution function during experiment with a pellet target, the particle dynamics was investigated numerically using Betacool program [5].

1.4. Brief description of numerical algorithms

Evolution of the proton (or deuteron) distribution function and particle number in time was simulated using Betacool program in the frame of Model Beam algorithm. In the Model Beam algorithm the proton beam is presented as an array of a few thousand of model particles. Dynamics of each model particle is simulated as a solution of Langevin equation in the momentum space. Each effect acting on ion distribution function is presented as a friction leading to regular variation of the particle momentum linearly with a step of integration over time, and diffusion leading to random variation of the momentum proportional to square root from the time step.

In experiment with internal target general effects leading to variation of the ion distribution function are electron and stochastic cooling, interaction with the target and intrabeam scattering.

For intrabeam scattering simulation the model proposed in [6] was used. Magnetized electron cooling leads to formation of dense core of the distribution function and for simulation of intrabeam

scattering in this case the “core-tail” model [7] was used. Stochastic cooling was simulated using model proposed by H.Stockhorst.

To compare possibilities of magnetized and non-magnetized electron cooling application the friction force in the electron beam was calculated using Binney formula [8] for non-magnetized case, Derbenev-Skrinsky [9] and Parkhomchuk’s formulae [10] for the magnetized one. All the formulae are presented in the Appendix to this report.

To simulate interaction with a pellet target a model based on calculation of the number of pellet crossings during integration step was developed. The model is described in the Appendix to this report.

2. ELECTRON COOLING SIMULATIONS

Simulations were done for parameters of proposed experiments with WASA internal target at COSY. The new electron cooler with the electron energy up to 2 MeV is under design now. The main parameters of simulation are presented in Table 2.1. For intrabeam scattering simulation the lattice structure of COSY shown in the Fig. 2.1 was used.

As it was shown in the previous chapter an electron cooling at realistic parameters can not suppress ionization energy loss on the dense target. However the luminosity life time can be sufficiently improved by the use an electron cooling in combination with usual RF or barrier RF bucket system. The bucket height has to be large enough to avoid particle loss after crossing the pellet. Real pellet density is a few orders of magnitude larger than an effective density which is used in estimations of the luminosity level. So the mean energy loss calculated from the effective thickness is equal to about 0.013 eV per single revolution in the ring, when the energy loss after single crossing the pellet is about 750 eV (Table 2.1). In the simulations of bunched beam presented here the RF voltage amplitude was chosen to be of 1 kV. At this value the rms bunch length is about 23 m and even for the particles from the tails of distribution function the losses from separatrix due to crossing the pellet are completely suppressed.

The beam bunching due to RF application leads to some increase of the beam heating due to intrabeam scattering. To estimate influence of intrabeam scattering on the beam dynamics the simulations were performed initially for a coasting beam without account of the mean energy loss (these simulations correspond to barrier bucket application at large bucket length) and then for a bunched beam with account of the mean energy loss.

General heating effects related to an interaction with internal target are intensity independent as well as the electron cooling and to estimate a time period required for reaching equilibrium the particle loss can be ignored. The beam life time is about a few thousands of seconds (Table 1.1) therefore the simulations at constant beam intensity slightly overestimate the luminosity. The simulations presented in the paragraphs two and three of this chapter has a goal to compare heating rate from the target with a cooling with magnetized or non-magnetized electron beam and the particle loss was not taking into account. In the forth paragraph the simulations of the luminosity were provided with account of all the effects.

Usual low energy electron cooling systems utilize a magnetic field of relatively large value for as an electron beam transportation as the electron magnetization to increase a friction force value. Below 300 keV of the electron energy the required value of the magnetic field is about 1 kG. At large electron energy the magnetic field value has to be increased also and requirements to the field quality are sufficiently stronger. Therefore the price of the magnetic system increases very fast with increase of the electron energy. To avoid this problem one can provide an electron cooling at large energy without magnetic field or at low value of the magnetic field. In this case the magnetic field does not influence on the friction force practically and the cooling process is described with so called “non magnetized” friction force.

First electron cooling system with non-magnetized electron beam is successfully operated at Recycler ring in Fermilab. The project of electron cooling system with non-magnetized electron beam is under development in BNL for RHIC. Current design of the high energy COSY electron cooler presumes magnetization of the electron beam and the field value in the cooling section is proposed to be of about 2 kG. One of the goals of this report is to investigate a possibility of non-magnetized cooling application at COSY energy range. The comparison of different cooling schemes is presented in the third paragraph of this chapter. The simulations were performed under assumption that the electron temperature in the cooling section has the same value in both cases.

Table 2.1. General parameters of the ring, electron cooling system and pellet target used in simulations

Beam parameters		
Momentum of proton [GeV/c]	3.7	
Proton energy, E [GeV]	2.884	
Relativistic factor, γ	4.09	
Initial emittance, ε [π mm mrad]	0.4	
Initial momentum spread	5×10^{-4}	
RF voltage [kV]	1	
Harmonic number	1	
Bunch length [m]	23.5	
Electron cooler		
Electron current, Ie [A]	0.1 ÷ 0.4	
Magnetic field, B [kG]	2	
Cooler length, Lc [m]	3	
Beta functions [m]	14 / 14	
Electron beam radius, a [cm]	0.5	
Electron temperature, Ttran / Tlong [eV]	0.3 / 0.01	
Homogeneity of magnetic field, $\Delta B/B$	10^{-5}	
Pellet target		
Density, $\Re$ [g/cm^3]	0.0708	
Flux radius, r_f [mm]	1	
Pellet size [μm]	25×25×25	
Mean distance between pellets [mm]	6	
Effective thickness [atoms/cm^2]	2×10^{15}	
Beta functions [m]	3 / 3	
Heating from pellet target	real density	effective
RMS scattering angle	5.56×10^{-6}	2.4×10^{-8}
Energy straggling [eV]	15675	67.9
Energy loss [eV]	744	0.013

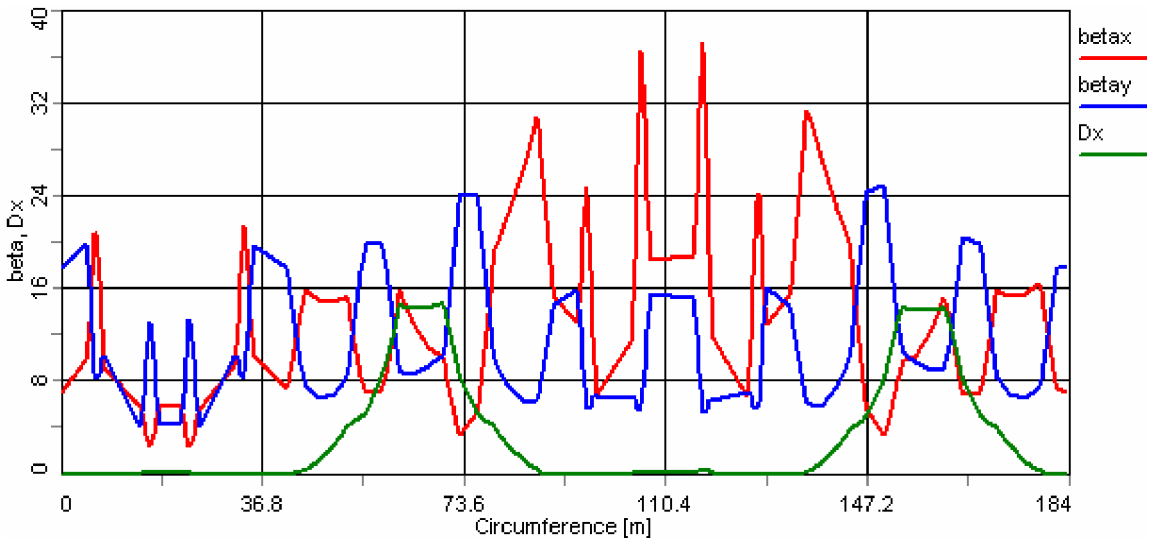

Fig. 2.1. Lattice parameters used in simulation of intrabeam scattering process.

2.1. Beam dynamics without cooling

From two processes limiting the luminosity life time (the particle losses and emittance growth) the emittance growth is dominating in experiment with a pellet target. For instance, at maximum COSY energy during 800 seconds of experiment the proton number decreases by about 10% only, when the luminosity decreases more than 1.5 times (Fig. 2.2). This effect is even more pronounced at the proton momentum of 2.25 GeV/c (Fig. 2.3). Here at the same experiment duration the luminosity decreases by about 2 times.

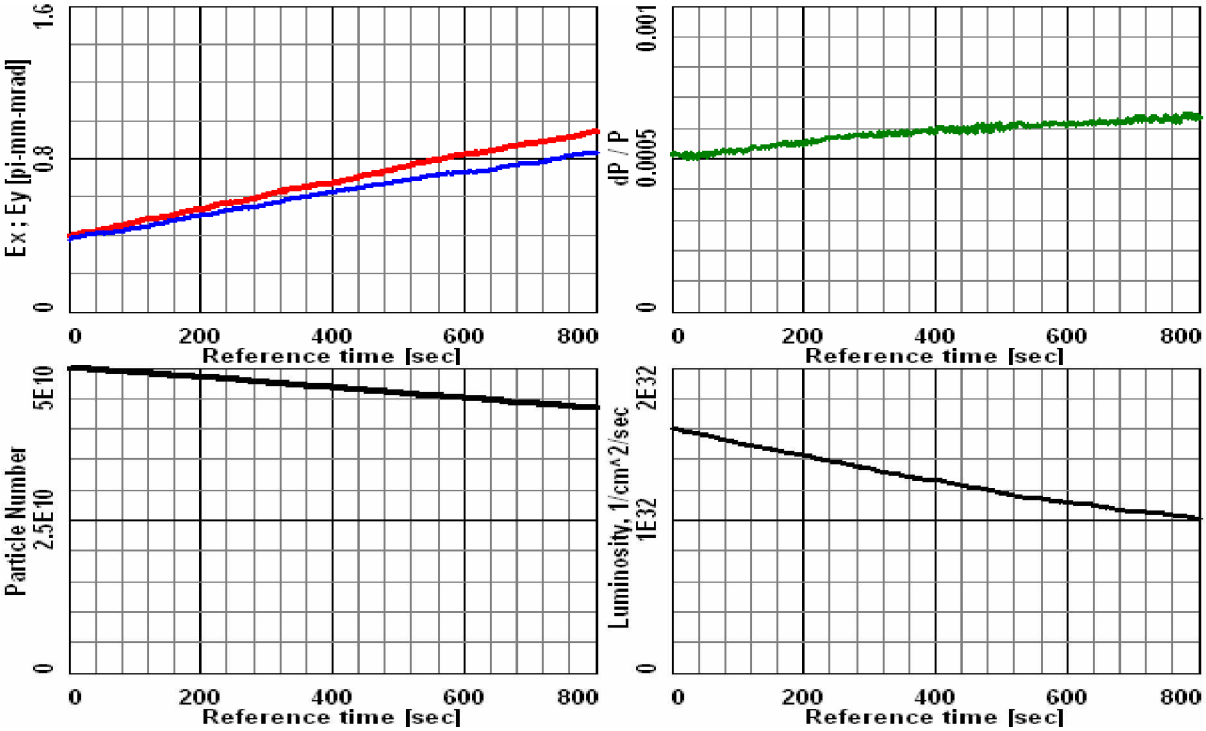

Fig.2.2. Evolution of beam parameter without cooling. Proton momentum is 3.7 GeV/c

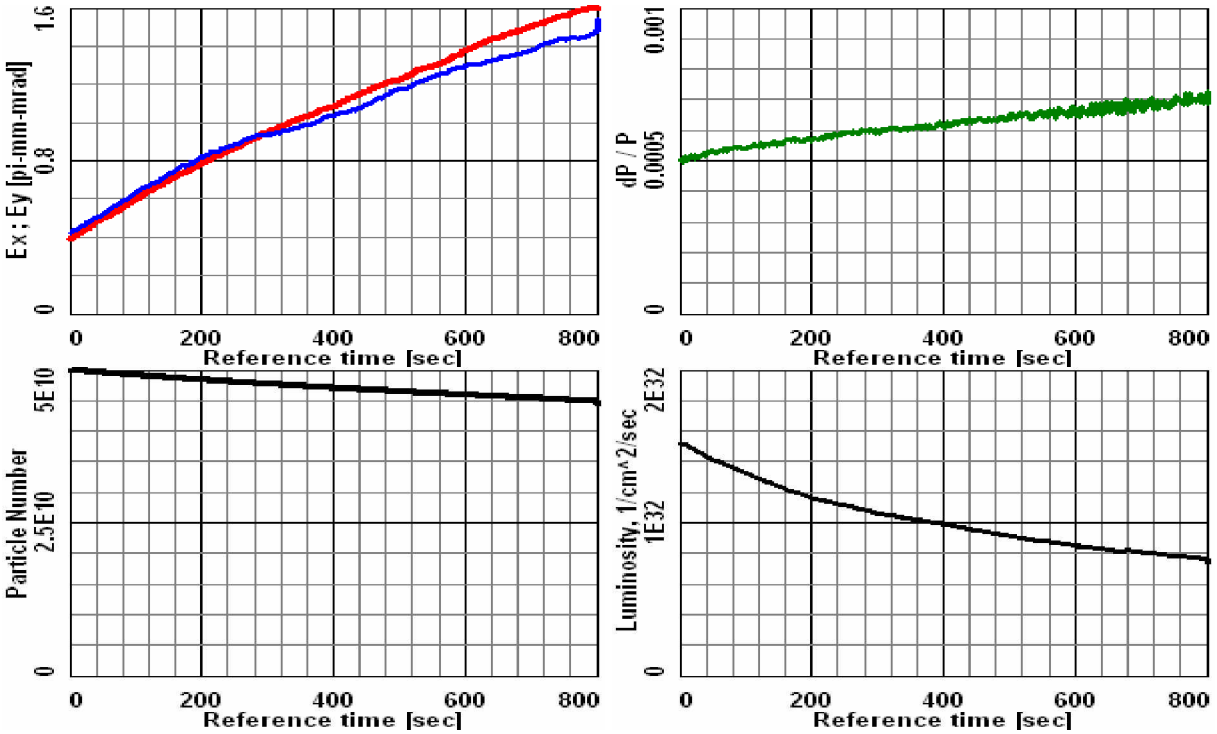

Fig.2.3. Evolution of beam parameter without cooling. Proton momentum is 2.25 GeV/c

The simulations presented in the Fig. 2.2 and 2.3 were performed for a bunched beam at RF amplitude of 1 kV.

Thus, a suppression of the emittance growth by a cooling application can give a gain in the average luminosity of about 2 times. Long experiment duration simplifies COSY operation and increases the experiment duty factor, which leads to additional gain in the average luminosity.

2.2. Magnetized cooling

Moderated estimation of the friction force acting on the ion inside magnetized electron beam can be done using semi-empirical formula proposed V.Parkhomchuk [9]. Parkhomchuk's formula is in good agreement with experimental measurements of the longitudinal component of the friction force performed at existing COSY cooling system as well as at a few others low energy coolers. In accordance with this formula (see chapter A.1.3 in appendix) the ion velocity corresponding to the force maximum and the force amplitude is determined by so called "effective" electron temperature, which depends mainly on temperature of longitudinal degree of freedom of electrons and magnetic field quality. In the simulations presented in this report we assumed that the relative field errors are equal to $\Delta B/B = 10^{-5}$. In this case the effective temperature coincides practically with the temperature of the longitudinal degree of freedom of the electrons (Table 2.1). The longitudinal temperature was estimated from the ripple of HV power supply assumed to be about $\Delta U/U = 10^{-4}$.

At large ion velocity the electron cooling rate depends on the beam emittance as

$$\frac{1}{\tau_{cool}} \sim \frac{1}{\varepsilon^{3/2}},$$

where the coefficient linearly scales with an electron current. The heating rate due to interaction with internal target at uniform thickness is proportional to

$$\frac{1}{\tau_{target}} \sim \frac{1}{\varepsilon}.$$

Therefore the equilibrium between cooling and heating is possible only starting from some minimum electron current value. The equilibrium conditions were investigated numerically in [11] using RMS dynamics algorithm. Here we present the results of dynamics simulations using Model Beam algorithm for two cases: coasting beam without account of mean energy loss (that corresponds to barrier bucket application at bucket length compared with the ring circumference) and bunched beam at 1 kV of RF amplitude.

For the coasting beam the minimum electron beam current required for compensation of the emittance growth and the energy straggling is about 300 mA (Fig.2.4). This value stabilizes practically the beam emittance and leads to insufficient decrease of the initial momentum spread.

The simulations of the bunched beam included the energy loss which was compensated by RF station. Because of slight increase of the intrabeam growth rate due to bunching the minimum electron beam current necessary for the emittance stabilization increases (Fig. 2.5). Practically constant emittance during long term experiment can be obtained at about 400 mA. However the ratio between longitudinal and transverse heating rates is distorted by intrabeam scattering and the electron current of 400 mA leads to decrease of the beam momentum spread by about 20%.

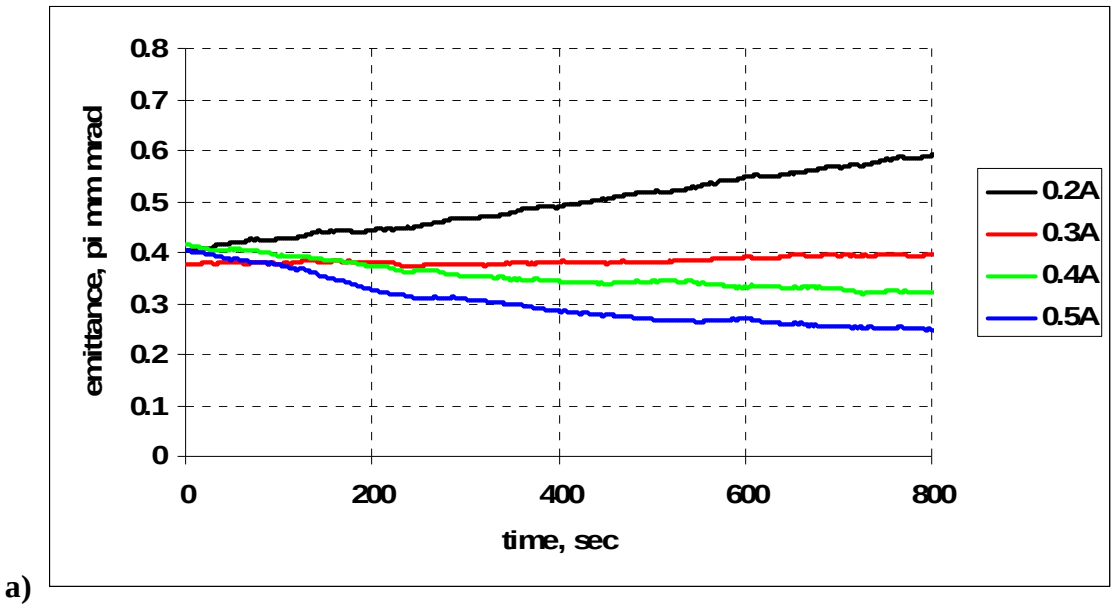

a)

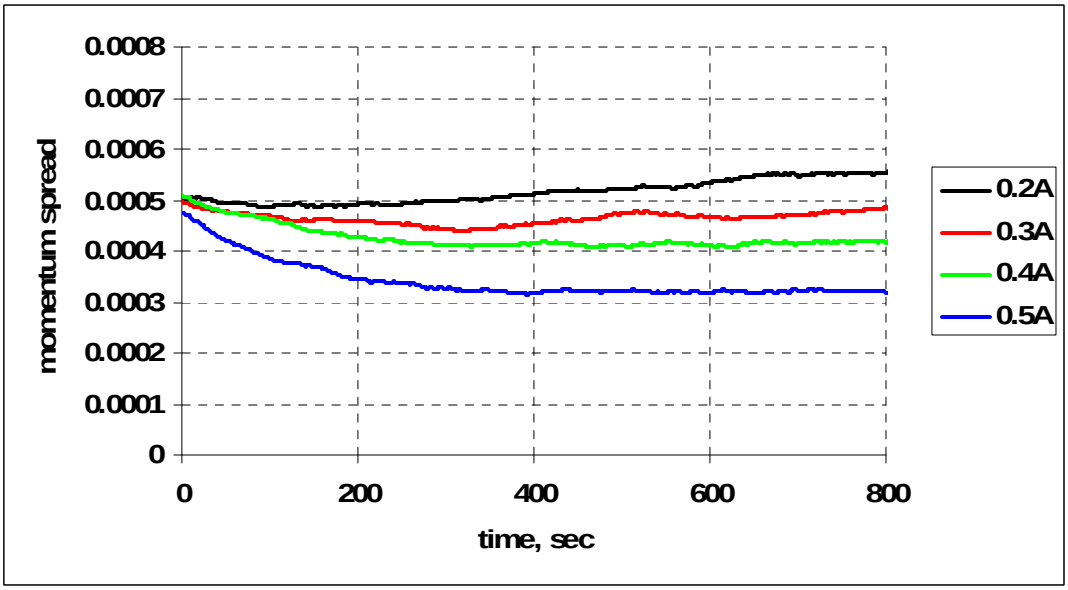

b)

Fig.2.4. The dependence of emittance (a) and momentum spread (b) for coasting beam on time for different values of electron beam current (Parkhomchuk model).

At the initial parameters of the proton beam listed in the Table 2.1 the luminosity is about 1.6×10^{32} $cm^{-2}s^{-1}$. Without account of the particle loss during the cooling process the luminosity increases with the decreas of transverse emittance (Fig.2.6). The luminosity depends on the transverse beam size due to finite transverse size of the pellet flux. At small emittance value, when the transverse size of the pellet flux is much more than the beam size, this dependence disappears. But for the target parameters listed in the Table 2.1 the beam emittance corresponding to this condition is about 0.1 π·mm·mrad. At such a value the transverse heating rate increases by about 2 times and required electron current increases also. Therefore the beam emittance of 0.4 π·mm·mrad seems to be optimum. In experiment the optimum beam emittance will be determined by real target geometry (flux radius, pellet dimensions, distance between pellets).

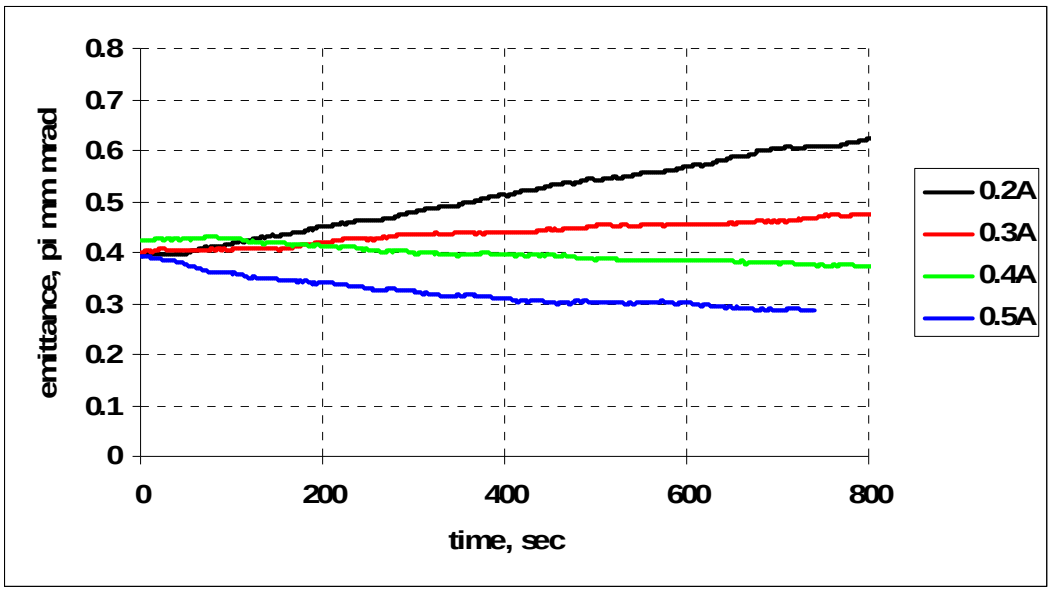

a)

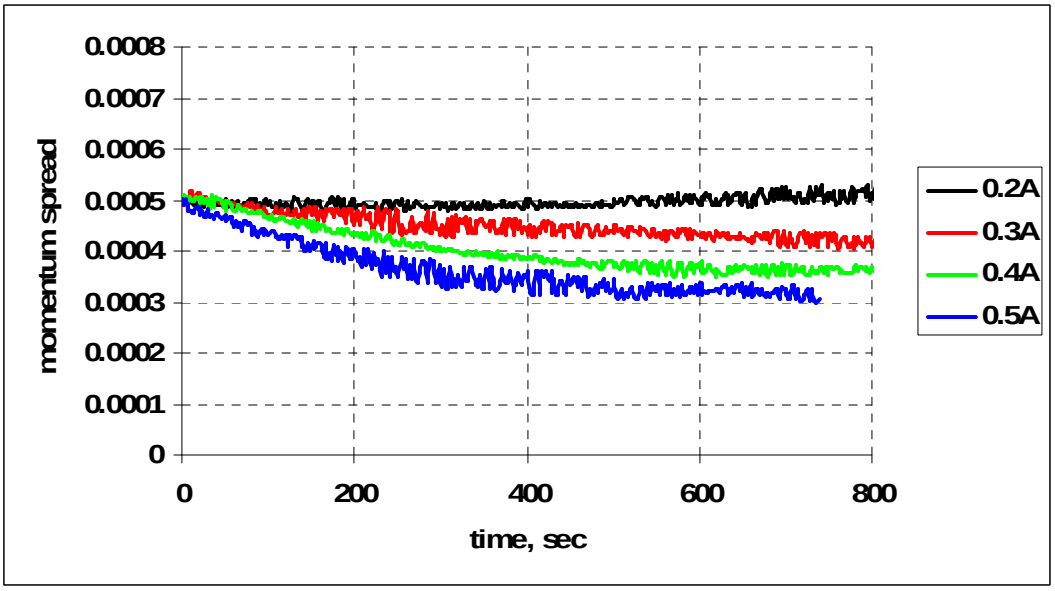

b)

Fig.2.5. The dependence of emittance (a) and momentum spread (b) for bunched beam on time for different values of electron beam current (Parkhomchuk model).

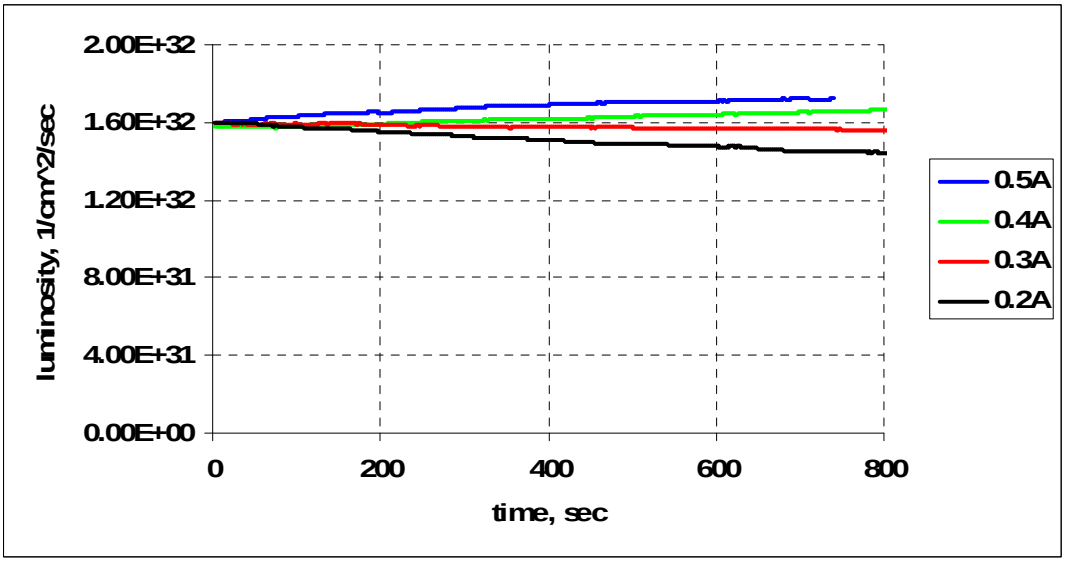

Fig.2.6. The dependence of luminosity for bunched beam on time for different values of electron beam current.

Sufficient peculiarity of the magnetized cooling is a formation of a dense core in the proton distribution function. This fact is illustrated in the Figure 2.7, where the beam profiles (left plot) and the ion distribution over invariants of the motion (right plot) after 800 sec of the cooling process are presented. About 60% particles are located inside the dense core and 40% in the long tails. The increase of the transverse rms emittance and momentum spread at small electron beam current (200-300 mA, Fig.2.4 and Fig.2.5) is related with a growth of the tails of the distribution function.

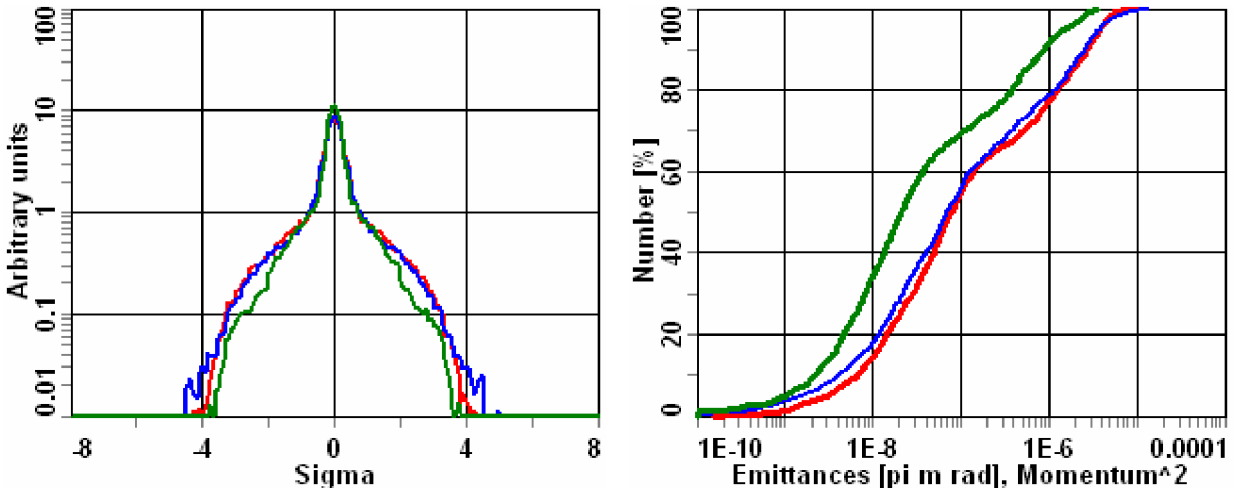

a) **b)**

Fig.2.7. Transverse (a, red and blue) and longitudinal (a, green) profiles and distribution of invariants (b) of cooled bunched beam (Ie =0.4 A).

2.3. Comparison of friction force models

Comparison between magnetized and non-magnetized cooling was performed assuming the same electron longitudinal and transverse temperatures in the both cases. In the case of non-magnetized electron beam the electron transverse temperature of 0.3 eV corresponds to the beam rms normalized emittance of about 2 π·mm·mrad which looks realistic for electrostatic accelerator.

The simulations in the previous paragraph were done using Parkhomchuk's formula for the friction force. This formula underestimates the longitudinal component of the friction force in comparison with formula derived in [8] by Derbenev and Skrinsky (Fig. 2.8). At parameters of the electron beam used in simulations the electron effective temperature is equal to longitudinal one practically, therefore the positions of the friction force maximum coincide in both models of magnetized force. The amplitudes of the transverse component of the friction force are almost equal in both models; therefore the luminosity (which depends on emittance and does not depend on momentum spread) has the same time-dependence.

Sufficient peculiarity of non-magnetized friction force relates with the fact that the position of the maximum of transverse component is shifted to the region of larger proton velocities. It leads to more effective cooling of the tails of the proton distribution function. As a result the non-magnetized cooling more effectively suppress the heating from the target, and the electron current required for the heating suppression is less than in the case of magnetized cooling. Simulation shows that for non-magnetized model of the friction force the minimum electron beam current is 200 mA that is by about two times less than for magnetized cooling (Fig.2.9). Correspondingly, the luminosity increases with the decrease of the transverse emittance (Fig.2.10.)

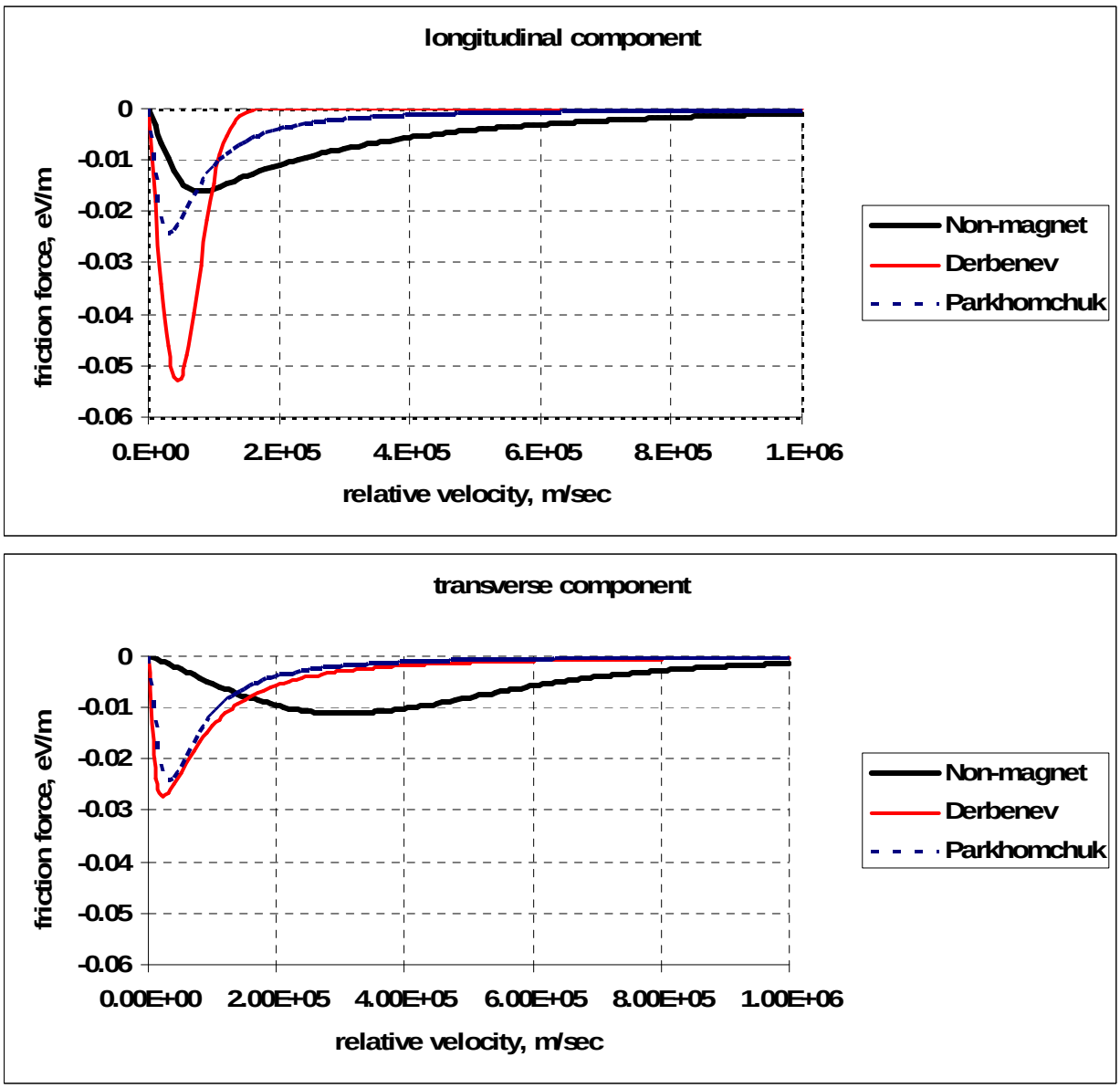

Fig.2.8. Ddependence of friction force components on the relative velocities between protons and electrons for different models of electron cooling (Ie=0.4A).

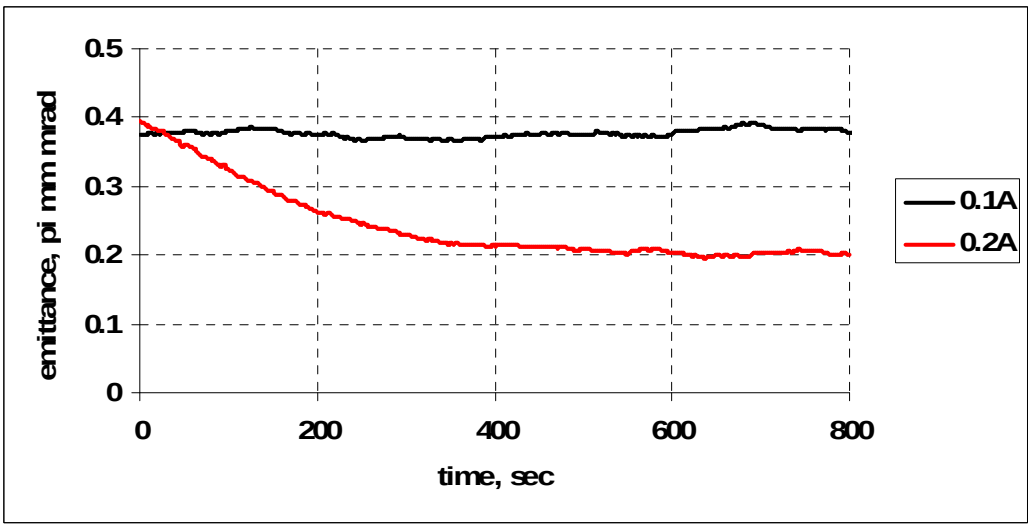

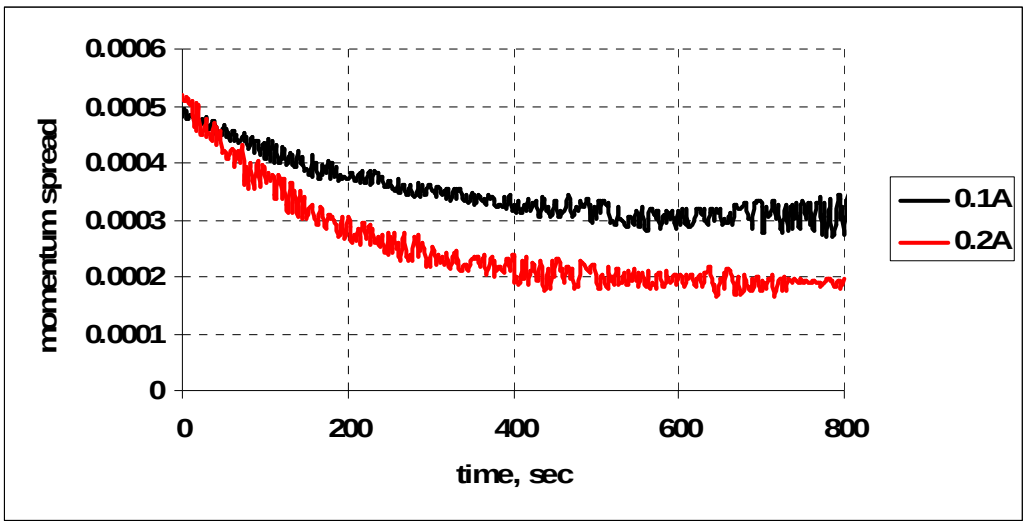

Fig.2.9. The dependence of emittance and momentum spread for bunched beam on time for different values of electron beam current (non-magnetize model).

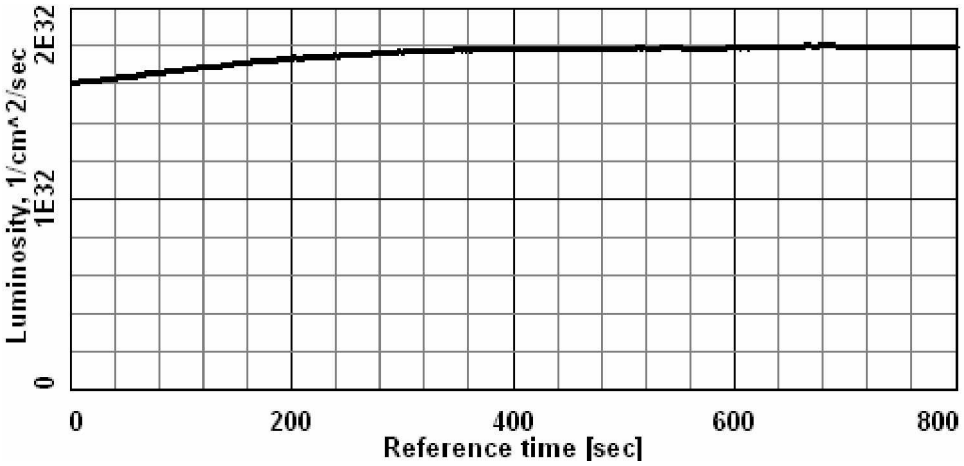

Fig.2.10. The dependence of luminosity for bunched beam on time at electron cooling (Ie=0.2A).

The beam profile after cooling during 800 sec has a large difference at magnetized (Fig.2.7) and non-magnetized friction forces (Fig.2.11). In the case of non-magnetized cooling only 10% particles are placed in tails but in the case of magnetized cooling the beam profile has more dense core of the beam distribution. It means that for parameters of WASA experiment at COSY the magnetized force more better cools the core of the proton beam and non-magnetized force – tails.

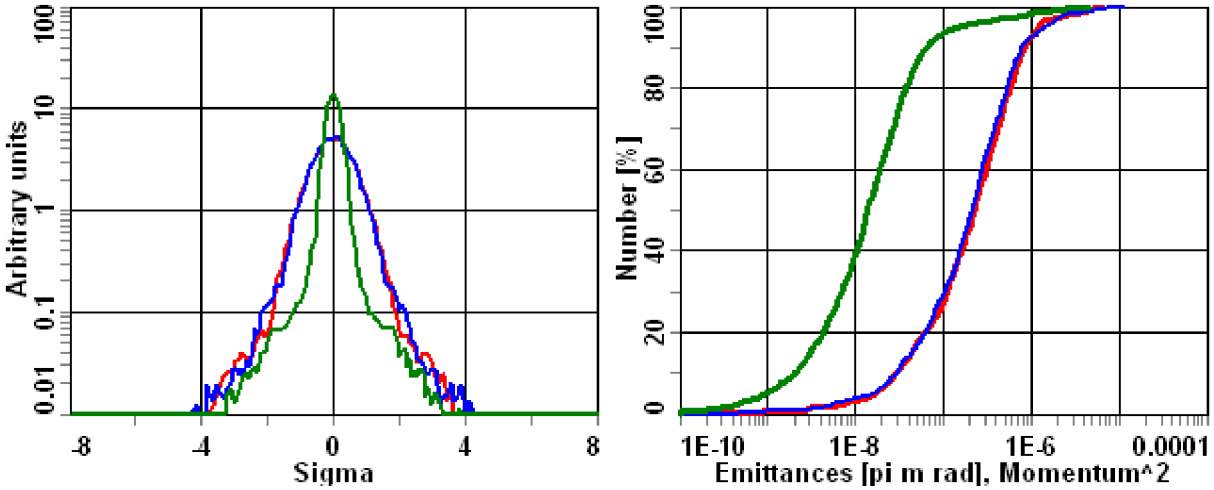

Fig.2.11. Transverse (a, red and blue) and longitudinal (a, green) profiles and sorted invariants (b) of cooled bunched beam (Ie =0.2 A)

2.4. Beam dynamics with particle losses

As it was shown in previous paragraphs an electron cooling system at realistic parameters can completely suppress the emittance growth due to interaction with a target and even to reduce the initial beam emittance by a few times. In absence of the particle loss the emittance decrease leads to increase of the luminosity (see Fig.2.6, 2.10). The particle loss is a competitive process to the emittance decrease and depending on cooling time the luminosity can be constant during experiment (Fig. 2.12) or vary in relatively small range (Fig. 2.13).

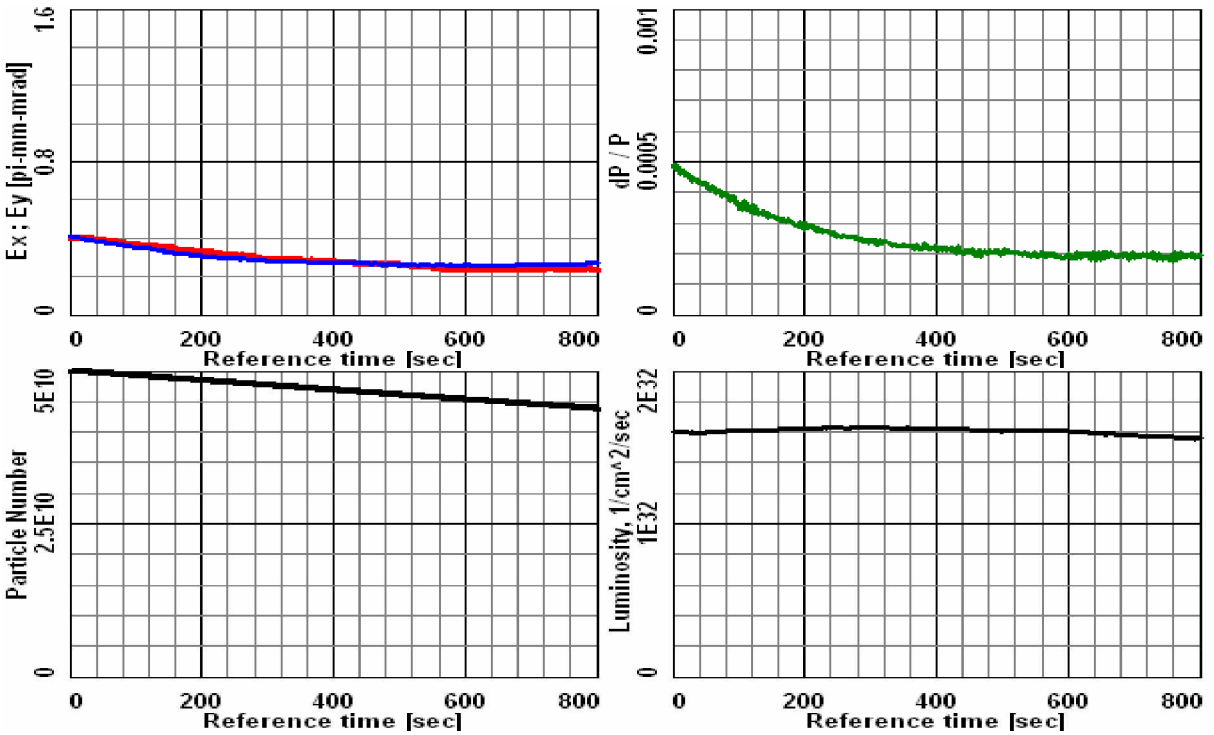

Fig.2.12. Evolution of beam parameter with electron cooling.
Non-magnetized cooling, Ie = 0.2 A, proton momentum is 3.7 GeV/c

At maximum COSY energy the time required for reaching an equilibrium is about 1000 seconds (Fig. 2.12). The decrease of emittance compensates the decrease of the particle number and the

luminosity does not changed significantly during this time. At small proton energy the same electron current corresponds to shorter cooling time (in the Fig. 2.13 the equilibrium is reached during about 100 seconds). In this case, the luminosity increases to some maximum value initially, because the decrease of emittance prevails on the particle loss. After that the emittance stays in equilibrium between cooling and heating processes and the luminosity decreases in accordance with decrease of the particle number.

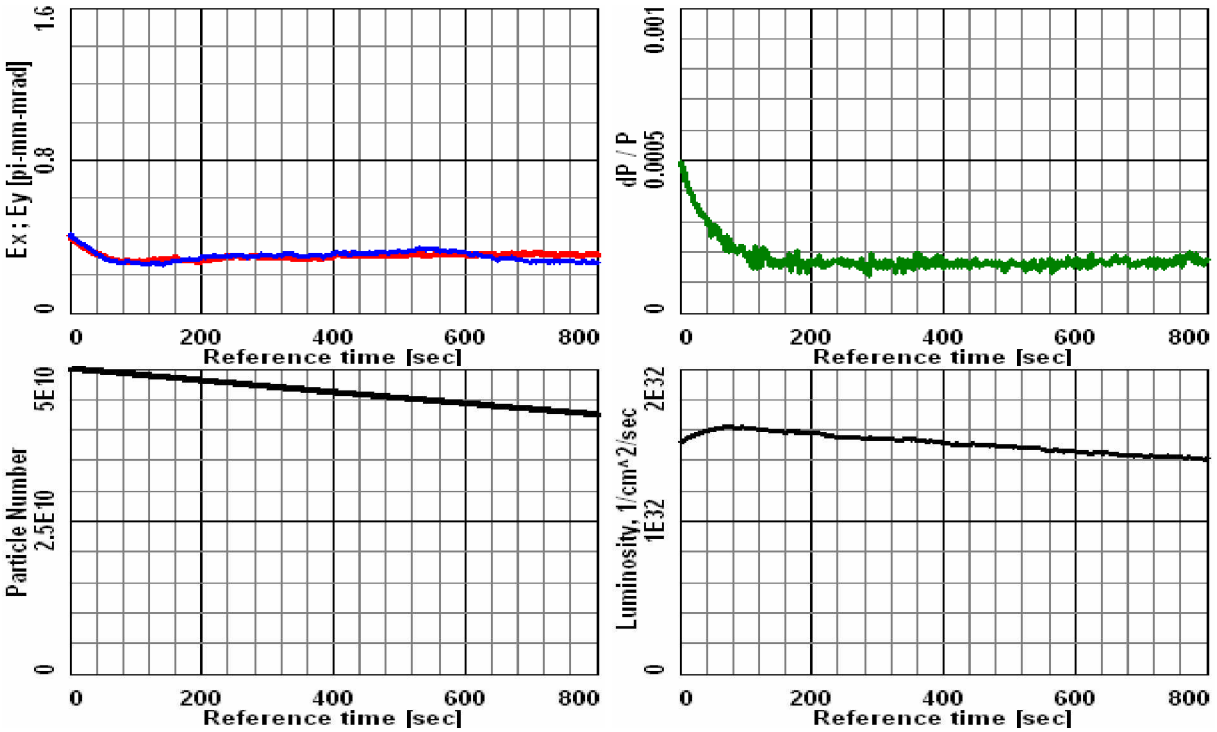

Fig.2.13. Evolution of beam parameter with electron cooling.
Non-magnetized cooling, Ie = 0.2 A, proton momentum is 2.25 GeV/c.

In principle, by variation of the electron current during experiment one can form the emittance time-dependence required for compensation of the particle loss and provide the experiment at constant luminosity.

3. STOCHASTIC COOLING APPLICATION FOR LUMINOSITY PRESERVATION

If the mean energy losses in the target are compensated by RF system the general effect limiting the experiment duration is the emittance growth due to multiple scattering with the target atoms. Increase of the horizontal emittance leads to decrease of the pellet target effective density and thus to decrease of the luminosity. The beam emittance can be stabilized by stochastic cooling application. In difference with an electron cooling the stochastic cooling rate does not depend practically on the beam emittance:

$$\frac{1}{\tau_{SC}} = \frac{1}{\varepsilon}\frac{d\varepsilon}{dt} \approx const \ , \tag{3.1}$$

but the heating rate determined by interaction with the target is inversely proportional to the beam emittance:

$$\frac{1}{\tau_{target}} = \frac{1}{\varepsilon}\frac{d\varepsilon}{dt} = \frac{\left(d\varepsilon / dt\right)_{target}}{\varepsilon} \tag{3.2}$$

because $\left(d\varepsilon / dt\right)_{target}$ is a constant depending on the target effective density. Therefore for each value of the target density the stochastic cooling suppresses the heating at some equilibrium emittance value equal to

$$\varepsilon_{eq} = \left(d\varepsilon / dt\right)_{target}\tau_{SC}. \tag{3.3}$$

Thus the stochastic cooling can be effectively applied up to the target effective density value corresponding to the equilibrium rms emittance below approximately the ring acceptance divided by six (at larger value one can expect sufficient particle loss on aperture).

More accurate simulation of stochastic cooling can be based on solution of Fokker-Plank equation tacking into account the friction dependence on the ion distribution and diffusion due to thermal noise power. In the frame of the model proposed by H.Stockhorst the transverse emittance derivative over time in each transverse plane is calculated as follows:

$$\frac{d\varepsilon}{dt} = -\frac{1}{\tau_{cool}}\left(\varepsilon - \varepsilon_{\infty}\right), \tag{3.4}$$

where τ_{cool} describes the drift term (friction) in the Fokker-Plank equation and the equilibrium emittance ε_{∞} (without another heating effects) corresponds to the diffusion term. The characteristic time of the emittance variation due to action of the stochastic cooling is equal:

$$\frac{1}{\tau} = \frac{1}{\varepsilon}\frac{d\varepsilon}{dt} = -\frac{1}{\tau_{cool}}\frac{\varepsilon - \varepsilon_{\infty}}{\varepsilon}. \tag{3.5}$$

The transverse cooling time is determined from the parameters of the cooling system as follows:

$$\frac{1}{\tau_{cool}} = \frac{16}{3}\frac{|\eta|\delta \cdot W^2}{Nf_0} \cdot xJ(x). \tag{3.6}$$

Here $\eta = \frac{1}{\gamma^2} - \frac{1}{\gamma_{tr}^2}$ is off-momentum factor of the storage ring, γ is Lorenz factor of the ion, γ_{tr} is critical energy of the ring in the rest energy units. f_0 is the ion revolution frequency. W = $f_{max} - f_{min}$ is the bandwidth of the system with lower frequency f_{min} and upper frequency f_{max}. N is the ion number. Total momentum spread of the beam δ is calculated from r.m.s. value in accordance with the shape of distribution function. For instance, at a parabolic distribution

$$\delta = 4\frac{\Delta p}{p_{rms}}. \tag{3.7}$$

Formfactor $xJ(x)$ is calculated through a frequency range as follows:

$$xJ(x) = x\left(1 - 2x\ln\left(\frac{x + f_{\max}/W}{x + f_{\min}/W}\right) + \frac{x^2}{(x + f_{\max}/W)(x + f_{\min}/W)}\right). \tag{3.8}$$

The x value is proportional to the linear gain of the system from pickup to kicker G_A :

$$x = G_A / R, \tag{3.9}$$

where the coefficient R is determined by parameters of pickup and kicker.

The equilibrium emittance value is determined by the cooling system parameters and the thermal noise power and a few orders of magnitude less than the beam emittance required in experiment. The ion momentum spread is changed very slightly during the experiment; therefore the transverse cooling rate can be rewritten as

$$\frac{1}{\tau_{SC}} \approx \frac{C_{SC}}{N}, \tag{3.10}$$

where C_{SC} is a constant during experiment.

The emittance value determined by equilibrium between scattering in the target and stochastic cooling corresponds to the equality:

$$\frac{1}{\tau_{target}} = \frac{1}{\tau_{SC}}. \tag{3.11}$$

The heating rate due to multiple scattering on the target atoms in accordance with (1.19) is equal to:

$$\frac{1}{\tau_{target}} = \frac{1}{\varepsilon_{x,y}}\frac{d\varepsilon_{x,y}}{dt} = \frac{\beta_{x,y}\theta_{rms}^2}{\varepsilon_{x,y}2T_{rev}}, \tag{3.12}$$

where the square of the scattering angle is linearly proportional to the target effective density

$$\theta_{rms}^2 = C_{target}\rho_{eff}. \tag{3.13}$$

The constant C_{target} depends on the target material and ion energy. For instance, for a hydrogen target and proton momentum of 3.7 GeV/c $C_{target} = 2.91 \cdot 10^{-31}$ cm^2.

Using luminosity definition (1.1) one can rewrite (3.12) as

$$\frac{1}{\tau_{target}} = \frac{\beta_{x,y} C_{target} L}{\varepsilon_{x,y} 2N}. \tag{3.14}$$

Substituting (3.14) and (3.10) into (3.11) one can find the equilibrium emittance value. It does not depend on the ion number and linearly proportional to the luminosity:

$$\varepsilon_{eq} = \frac{\beta_{x,y} C_{target}}{2C_{SC}} L. \tag{3.15}$$

COSY vertical acceptance is less than the horizontal one and maximum luminosity achievable with stochastic cooling application in long-term experiment can be estimated as:

$$L_{\max} = \frac{A_y C_{SC}}{3\beta_y C_{target}}. \tag{3.16}$$

At 10^{10} protons at momentum of 3.7 Gev/c and the momentum spread of $5 \cdot 10^{-4}$ the formula (3.6) gives the cooling time of about 50 sec at optimum gain for the stochastic cooling system at bandwidth of 2 GHz and lower frequency of 1 GHz. It corresponds to the stochastic cooling constant of $C_{SC} = 2 \cdot 10^8$ s^{-1} and in accordance with (3.16) the maximum achievable luminosity is equal to about $1.5 \cdot 10^{33}$ cm^{-2}s^{-1}. To reach this value at the beam emittance of about $4 \cdot 10^{-6}$ π·m·rad one needs to sufficiently increase of the real target density (for instance by increase of the pellet radius). In this case one can expect very fast heating of the central part of the beam and sufficient deviation of the proton distribution from Gaussian. At such parameters the beam dynamics was investigated using Model Beam algorithm.

Numerical simulation of the beam dynamics were performed at the the pellet sizes of 70×70×70 μm. Initial beam emittance was chosen to be 3 π·mm·mrad in both transverse planes. All the other parameters were the same as in the Table 2.1. To compensate the mean energy loss an RF voltage of 1 kV is applied at the first harmonics of revolution frequency. Stochastic cooling was used for transverse degrees of freedom, the bandwidth is 2 GHz and lower frequency is 1 GHz, the electronic gain was chosen to be optimum at initial beam parameters. Intrabeam scattering and particle loss during interaction with the target were taken into account.

At these parameters initial luminosity is $1.6 \cdot 10^{33}$ cm^{2}s^{-1}. Without transverse cooling the particle losses on vertical aperture are started within a few seconds and during 150 seconds luminosity decreases by two times. The transverse stochastic cooling stabilizes the beam emittance (Fig. 3.1) as it predicted by the formula (3.15). Thereafter because of decrease of the proton number and increase of the momentum spread the cooling rate increases. The beam emittance begin to decrease that compensate decrease of the proton number and it stabilizes the luminosity at the level of about $1.4 \cdot 10^{33}$ cm^{2}s^{-1}. Because of strong dependence of the target effective density on the horizontal emittance the proton distribution in horizontal plane deviates sufficiently from Gaussian shape (Fig. 3.2). The experiment duration in this case is limited by increase of the momentum spread.

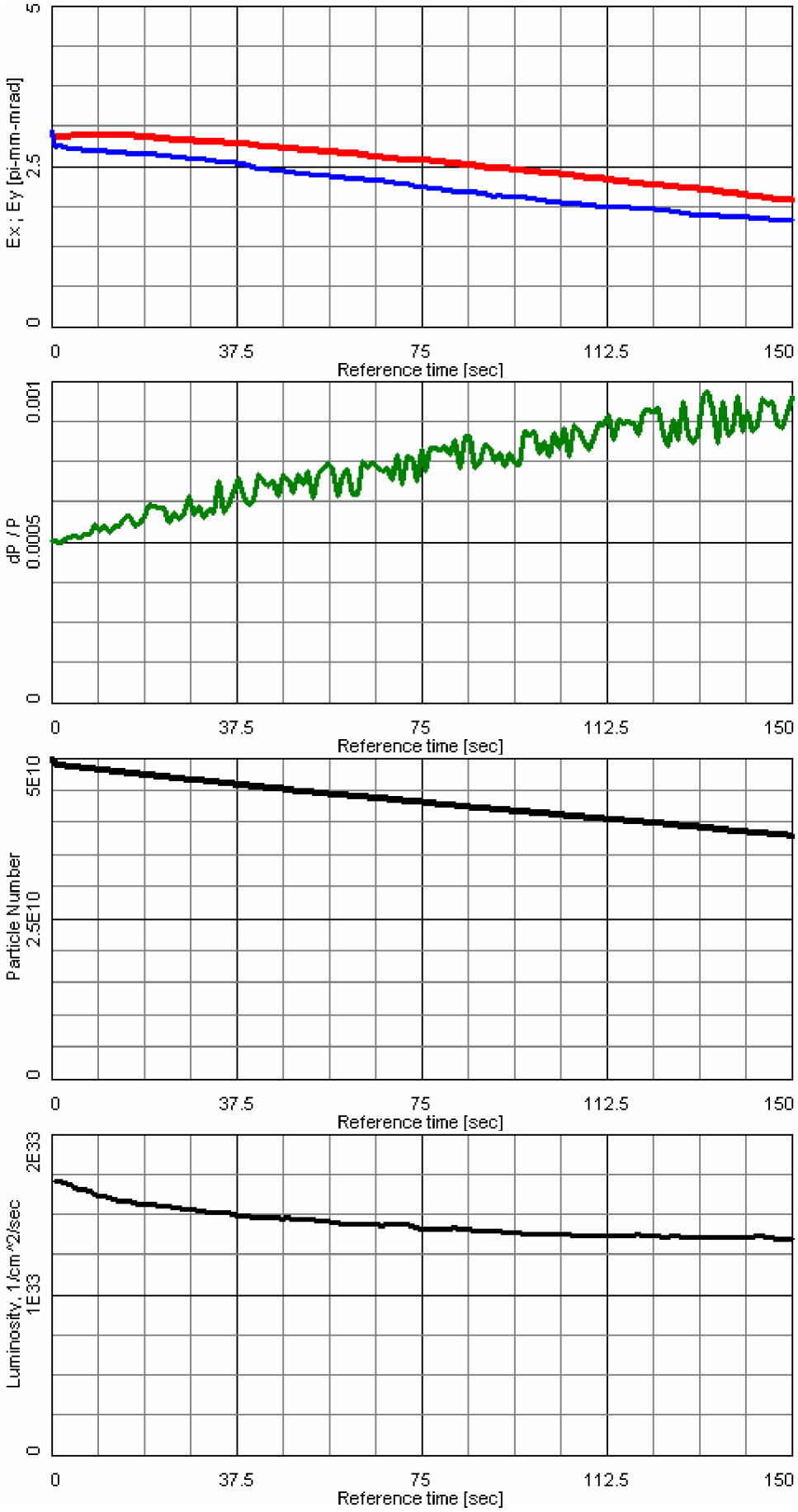

Fig. 3.1. From top to bottom: evolution of the beam emittance, momentum spread, proton number and luminosity under the common action of internal target, intrabeam scattering and transverse stochastic cooling. Initial effective target thickness is $1.3 \cdot 10^{16}$ Atoms/cm^2.

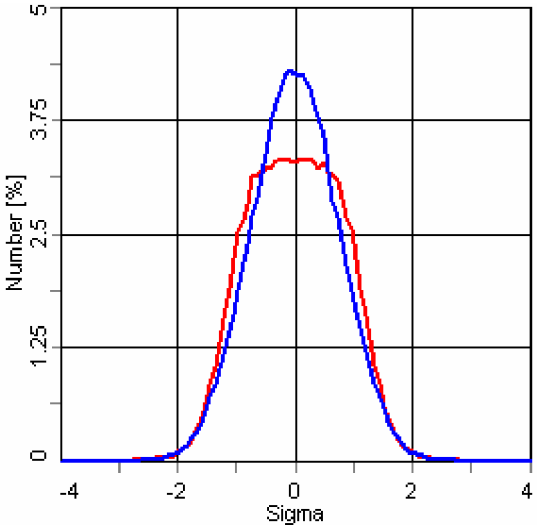

Fig. 3.2. Horizontal (red curve) and vertical (blue curve) beam profiles after 150 seconds of experiment. Initial effective target thickness is $1.3 \cdot 10^{16}$ Atoms/cm^2.

Thus the stochastic cooling application can stabilize the luminosity even at extremely large value. The estimation of the achievable luminosity in long term experiment can be done for some optimum equilibrium emittance value:

$$L = \frac{2\varepsilon_{opt} C_{SC}}{\beta_{x,y} C_{target}}, \tag{3.17}$$

and the optimum emittance can be chosen from the condition

$$\sigma_x \approx r_f, \tag{3.18}$$

where σ_x is the rms horizontal dimension of the beam and r_f is the pellet flux radius. At the beta function of 3 m the beam emittance corresponding to (3.18) is about 0.4 π·mm·mrad and the luminosity value determined by (3.17) is equal to about $1.6 \cdot 10^{32}$ cm^{-2}s^{-1}. The pellet size in this case is the same as in simulations presented in the part 2.

As it predicted by the formula (3.17) initially the stochastic cooling stabilizes the beam emittance (Fig. 3.3). Thereafter because of decrease of the particle number and increase of the momentum spread the cooling rate increases that leads to decrease of the beam emittance. The luminosity stays constant practically during more than 800 sec of experiment. The experiment duration (as in previous case) is limited by increase of the momentum spread and can be chosen of 1000 – 2000 sec.

Thus the simulations of stochastic cooling based on formula (3.6) shows that the power of existing cooling system is big enough to provide stabilization of the beam emittance at optimum value and the achievable luminosity level is closed to design parameters. The formula (3.6) is based on some approximation of real cooling system. More realistic estimations can be obtained by experimental investigation of the stochastic cooling system. For this goal one can measure the cooling time at known beam intensity, or measure equilibrium beam emittance in experiment with internal target at known luminosity. The stochastic cooling constant can be calculated using formula (3.10) in the first case or formula (3.15) in the second case.

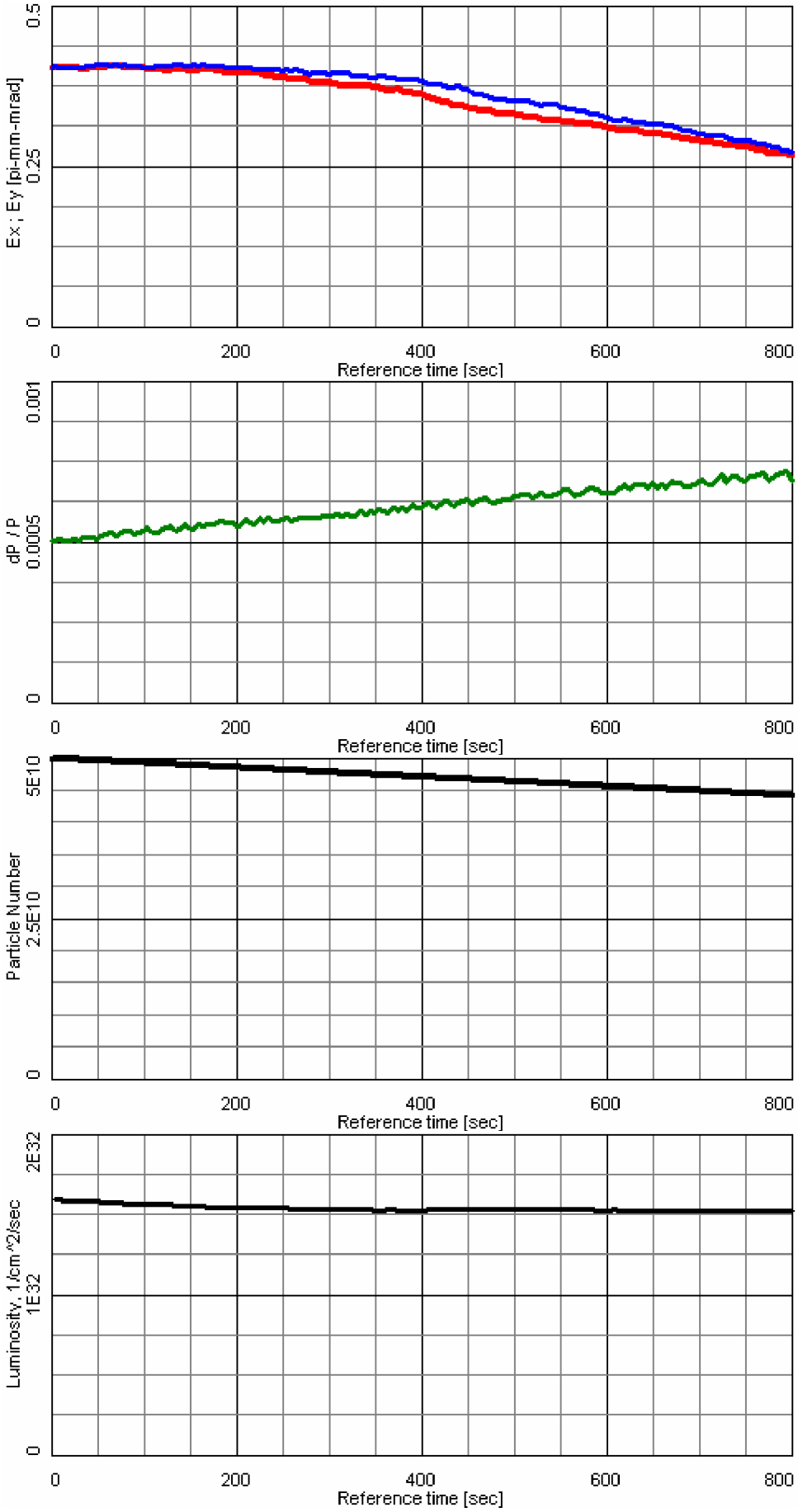

Fig. 3.3. From top to bottom: evolution of the beam emittance, momentum spread, proton number and luminosity under the common action of internal target, intrabeam scattering and transverse stochastic cooling. Initial effective target thickness is $2 \cdot 10^{15}$ Atoms/cm^2.

CONCLUSIONS

General effect limiting the beam on target time in experiment with internal target is ionization energy losses. At the target density of $2 \cdot 10^{15}$ Atoms/cm^2 the experiment time can be equal to a few minutes. To suppress this process the power of electron or stochastic cooling has to be unrealistic large.

The mean energy losses can be compensated by application of sinusoidal RF or Barrier RF bucket at relatively small amplitude. In this case the experiment time is limited mainly by the particle loss due to inelastic scattering in the target. The beam heating leading to increase of the beam emittance and momentum spread is slow process, and experiment can be provided without cooling during about one hour.

The last conclusion is related to a target with uniform density. In the case of pellet target the luminosity depends on the beam emittance because of finite dimensions of the pellet flux. Suppression of the emittance growth by a cooling application is necessary to provide experiment during a long time.

Effective thickness of the pellet target strongly depends on the horizontal emittance. To avoid sufficiently different heating rates for the particles in the beam core and in the tails the horizontal rms emittance has to lie between 0.1 and 0.4 π·mm·mrad. Therefore before beginning of the experiment the initial emittance has to be decreased by about 20 times. The beam precooling can be done using electron cooling at injection energy or stochastic/electron cooling at energy of experiment.

Numerical simulations performed using Betacool program shown that at maximum energy of COSY beam and at the beam intensity of about $5 \cdot 10^{10}$ particles the heating can be effectively suppressed by both – an electron or stochastic cooling. At the beam momentum of 2.25 GeV/c the stochastic cooling system efficiency decreases because of small momentum slip factor. The possibility of stochastic cooling operation together with RF system can not be investigated in the frame of existing numerical model.

In the linear approximation a stochastic cooling system can always suppress a heating due to interaction with a target. However the equilibrium emittance increases with increase of the luminosity. The maximum achievable luminosity corresponds to equilibrium emittance equal to the ring acceptance. At the parameters of existing stochastic cooling system the maximum luminosity exceeds 10^{33} cm^{2}s^{-1}. At the design luminosity level the beam emittance can be stabilized at the level of 0.4 π·mm·mrad. More accurate estimation can be done after experimental investigation of the cooling system.

An electron cooling can suppress the emittance growth due to interaction with an internal target starting from some minimum value of an electron current. It caused by sufficient nonlinearity of the friction force. At design luminosity level the proposed high energy electron cooling system can suppress the heating due to interaction with a pellet target at the electron current of $I_e \geq$ 200÷400 mA in the total energy range.

Comparison between magnetized and non-magnetized electron cooling shown that the non-magnetized cooling effectively cools down “the tails” of the beam distribution and provides the same cooling power as magnetized one at even less current.

Experimental investigation of the friction force in electron cooler in both cases – magnetized and non-magnetized - can be provided at existing cooling system.

Thus, when the ionization energy losses are compensated by RF system, the application of electron or stochastic cooling permits to provide the experiment at WASA target during about 1000 seconds without sufficient decrease of the luminosity. Expected gain in the average luminosity due to cooling application is by 2 – 3 times.

At maximum COSY energy the application of stochastic cooling seems more attractive because it permits to achieve high level of the luminosity. However the stochastic cooling can not be effectively operated in the total energy range required for experiments, and one needs to demonstrate a possibility of the system operation together with RF. Electron cooling system at design parameters can provide required luminosity level in the total energy range at reasonable electron current value. Both systems are complimentary to each other and one of them or both together can be operated depending on experiment conditions.

REFERENCES

1. Proposal for the Wide Angle Shower Apparatus (WASA) at COSY-Juelich "WASA at COSY" Juelich, October 5, 2004
2. J. Dietrich, V.V. Parkhomchuk, THE PROPOSED 2 MEV ELECTRON COOLER FOR COSY-JUELICH, Proceedings of EPAC 2006, Edinburgh, Scotland, 1684.
3. A. Lehrach, D. Prasuhn, Luminosity Considerations for Internal and External Experiments @ COSY, Annual Report of the IKP 2003
4. F. Hinterberger, D.Prasuhn, Analysis of internal target effects in light ion storage ring, NIM A 279(1989), 413-422
5. I.N.Meshkov, A.O.Sidorin, A.V.Smirnov, E.M.Syresin, G.V.Trubnikov, P.R.Zenkevich, "Simulation of Electron Cooling Process in Storage Rings Using BETACOOL Program" , Proceedings of Beam Cooling and Related Topics, Bad Honnef, Germany, 2001.
6. M. Martini “Intrabeam scattering in the ACOOL-AA machines”, CERN PS/84-9 AA (1984).
7. I. Meshkov, A. Sidorin, A. Smirnov, G. Trubnikov, A. Fedotov, Physics guide of BETACOOL code, C-A/AP/#262 November 2006, http://www.agsrhichome.bnl.gov/AP/ap_notes/ap_note_262.pdf
8. J. J. Binney, MNRAS 181, p. 735 (1977).
9. Ya.S. Derbenev and A.N. Skrinsky, Fyzika plasmy, 1978. v.4, p.492; Part. Accelerators 8, p. 235 (1978).
10. V. Parkhomchuk, New insights in the theory of electron cooling, NIM A 441 (2000) 9-17, p.9.
11. I.Meshkov, R.Maier, et al, Electron cooling application for luminosity preservation in an experiment with internal targets at COSY, ISSN 0944-2952, Institute fuer Kernfhysik, Juel-4031, 2003.

APPENDIX
FRICTION FORCE FORMULAE AND PELLET TARGET MODEL

A.1. Electron cooling

A.1.1. Non-magnetize cooling

In the frame of binary collision model, when the electrons are distributed over velocities in accordance with the function $f(v_e)$, the friction force in the particle frame can be evaluated by numerical integration of the following formula

$$\overset{\circ}{F} = -\frac{4\pi n_e e^4 Z^2}{m} \int \ln\left(\frac{\rho_{\max}}{\rho_{\min}}\right) \frac{V - \overset{\smile}{v_e}}{\left|V - v_e\right|^3} f(v_e) d^3 v_e, \qquad \text{(A.1.1)}$$

where V is the ion velocity. The Coulomb logarithm $\ln\frac{\rho_{\max}}{\rho_{\min}}$ is kept under the integral because the minimal impact parameter depends on electron velocity:

$$\rho_{\min} = \frac{Ze^2}{m} \frac{1}{\left|V - v_e\right|^2}. \qquad \text{(A.1.2)}$$

At given value of the ion velocity the maximum impact parameter is constant and it is determined by dynamic shielding radius or the ion time of flight through the electron cloud. Radius of the dynamic shielding sphere coincides with Debay radius:

$$\rho_D = \frac{\Delta_e}{\omega_p}, \qquad \text{(A.1.3)}$$

when the ion velocity is less than the electron r.m.s velocity spread Δ_e. The plasma frequency ω_p is equal to

$$\omega_p = \sqrt{\frac{4\pi n_e e^2}{m}}. \qquad \text{(A.1.4)}$$

When the ion velocity sufficiently larger than the electron velocity spread it determines the shielding radius

$$\rho_{sh} = \frac{V}{\omega_p}. \qquad \text{(A.1.5)}$$

The both formulae (A.1.3) and (A.1.5) can be combined together to have a smooth dependence of the shielding radius on the ion velocity:

$$\rho_{sh} = \frac{\sqrt{V^2 + \Delta_e^2}}{\omega_p}. \qquad \text{(A.1.6)}$$

In the case, when the shielding sphere does not contain big enough number of electrons to compensate the ion charge (such a situation takes a place in the case of magnetized electron beam at low longitudinal velocity spread) it has to be increased in accordance with the electron beam density and the ion charge. In the program this radius is estimated from the expression

$$n_e \rho^3 \sim 3Z\,. \tag{A.1.7}$$

As a result, the maximum impact parameter is calculated as a minimum from three values:

$$\rho_{\max} = \min\left\{\max\left(\rho_{sh},\ \sqrt[3]{\frac{3Z}{n_e}}\right), V\tau\right\}. \tag{A.1.8}$$

The second term describes the distance, which the ion passes inside the electron beam. Here τ is the ion time of flight the cooling section in the PRF:

$$\tau = \frac{l_{cool}}{\beta\gamma c}\,. \tag{A.1.9}$$

In the case of axial symmetry the electron distribution function can be written in the following form:

$$f(v_e) = \left(\frac{1}{2\pi}\right)^{3/2} \frac{1}{\Delta_\perp^2 \Delta_\parallel} \exp\left(-\frac{v_\perp^2}{2\Delta_\perp^2} - \frac{v_\parallel^2}{2\Delta_\parallel^2}\right), \tag{A.1.10}$$

where $\Delta_\perp$ and $\Delta_\parallel$ are the electron rms velocity spreads in the transverse and longitudinal direction correspondingly.

At the ion velocity $V >> \Delta_\parallel, \Delta_\perp$ the minimal impact parameter becomes to be constant:

$$\rho_{\min} = \frac{Ze^2}{m_e} \frac{1}{V_\perp^2 + V_\parallel^2}\,, \tag{A.1.11}$$

and Coulomb logarithm can be removed from the integral. At extremely small ion velocity the calculation of the minimal impact parameter in accordance with the formula (A.1.11) leads to zero friction force value, when becomes to be $\rho_{\min} > \rho_{\max}$. One can avoid this problem introducing mean minimal impact parameter in accordance with

$$\rho_{\min} = \frac{Ze^2}{m_e} \frac{1}{V_\perp^2 + V_\parallel^2 + \Delta_\perp^2 + \Delta_\parallel^2}\,. \tag{A.1.12}$$

When the Coulomb logarithm L_C is constant the two of three integrals in (A.1.1) can be calculated analytically and the friction force components can be written in accordance with Binney's formulae[7]:

$$F_\perp = 2\sqrt{2\pi}\, \frac{n_e e^4 Z^2 L_C}{m} \frac{V_\perp}{\Delta_\perp^3} B_\perp$$

$$F_{\parallel} = 2\sqrt{2\pi}\,\frac{n_e e^4 Z^2 L_C}{m}\,\frac{V_{\parallel}}{\Delta_{\perp}^3}\,B_{\parallel}, \tag{A.1.13}$$

where $B_{\perp}$ and $B_{\parallel}$ are the following integrals:

$$B_{\perp} = \int_0^{\infty} \frac{\exp\left(-\dfrac{V_{\perp}^2}{2\Delta_{\perp}^2}\dfrac{1}{1+q} - \dfrac{V_{\parallel}^2}{2\Delta_{\perp}^2}\dfrac{1}{\left(\Delta_{\parallel}/\Delta_{\perp}\right)^2+q}\right)}{(1+q)^2\left(\left(\Delta_{\parallel}/\Delta_{\perp}\right)^2+q\right)^{1/2}}dq,$$

$$B_{\parallel} = \int_0^{\infty} \frac{\exp\left(-\dfrac{V_{\perp}^2}{2\Delta_{\perp}^2}\dfrac{1}{1+q} - \dfrac{V_{\parallel}^2}{2\Delta_{\perp}^2}\dfrac{1}{\left(\Delta_{\parallel}/\Delta_{\perp}\right)^2+q}\right)}{(1+q)\left(\left(\Delta_{\parallel}/\Delta_{\perp}\right)^2+q\right)^{3/2}}dq. \tag{A.1.14}$$

A.1.2. Magnetized cooling, Derbenev-Skrinsky formulae

In the magnetized electron beam, when the maximum impact parameter (A.1.8) is larger than radius of electron Larmor rotation the magnetized collisions between ion and electron take place. In this case the electron is attracted by the ion, which pulls it along the magnetic field line forth or back, depending on the ion position [8]. In different ranges of the ion velocity and impact parameter three type of collisions are possible: fast, adiabatic and magnetized.

Magnetized collisions

At ion collisions with electrons at the impact parameter higher than the mean radius of electron Larmor rotation

$$\rho_{\perp} = \frac{cm\Delta_{\perp}}{eB} \tag{A.1.15}$$

the friction force in the particle rest frame can be expressed as follows [3]:

$$\overset{\circ}{F} = \frac{2\pi Z^2 e^4 n_e}{m}\,\frac{\partial_{\circ}}{\partial V}\int\left[\frac{V_{\perp}^2}{U^3}L_M + \frac{2}{U}\right]f(v_e)dv_e, \tag{A.1.16}$$

where $U = \sqrt{V_{\perp}^2 + \left(V_{\parallel} - v_e\right)^2}$ - the relative velocity of the ion and electron "Larmor circle". $f(v_e)$ is the electron distribution over longitudinal velocity, in the case of Maxwellian distribution with rms velocity spread of $\Delta_{\parallel}$ it is expressed as

$$f(v_e) = \frac{1}{\sqrt{2\pi}\Delta_{\parallel}}\exp\left(-\frac{v_e^2}{2\Delta_{\parallel}^2}\right). \tag{A.1.17}$$

Maximum impact parameter in the Coulomb logarithm for magnetized collisions

$$L_M = \ln\left(\frac{\rho_{\max}}{\rho_{\perp}}\right) \tag{A.1.18}$$

is calculated as usual (A.1.8).

Friction force at small impact parameters

When the impact parameter is less than the radius of the electron rotation $\rho < \rho_\perp$ the influence of the magnetic field can be neglected and the friction force can be calculated in accordance with:

$$\overset{\circ}{F} = -\frac{4\pi n_e e^4 Z^2}{m} \int \left(L_F + N_{coll} L_A\right) \frac{\overset{\circ}{V} - \overset{\circ}{v}_e}{\left|\overset{\circ}{V}_i - \overset{\circ}{v}_e\right|^3} f(v_e) d^3 v_e . \qquad \text{(A.1.19)}$$

The range of impact parameters from ρ_{min} to $\rho_\perp$ in (A.1.19) is divided by two regions: the region where

$$\rho_{min} < \rho < \rho_F$$

corresponds to so called “fast collisions” and in the region of

$$\rho_F < \rho < \rho_\perp$$

the ion can collide with the same electron a few times during its movement through the cooling section. The last region corresponds to so called “adiabatic” or “cycling” collisions. The intermediate impact parameter ρ_F is equal to:

$$\rho_F = \rho_\perp \frac{\sqrt{V^2 + \Delta_\parallel^2}}{\Delta_\perp}, \qquad \text{(A.1.20)}$$

and corresponding Coulomb logarithms are:

$$L_A = \ln \frac{\rho_\perp}{\rho_F}, \; L_F = \ln \frac{\rho_F}{\rho_{min}}. \qquad \text{(A.1.21)}$$

The number of multiple adiabatic collisions of the ion with the same electron is [4]:

$$N_{coll} = 1 + \frac{\Delta_\perp}{\pi \sqrt{V^2 + \Delta_\parallel^2}}. \qquad \text{(A.1.22)}$$

Numerical evaluation of the integral (A.1.19) is discussed in the chapter dedicated to nonmagnetized cooling.

A.1.3. Semi-empirical formula by Parkhomchuk

In [9] was proposed a semi-empirical formula for calculation of the friction force in magnetized electron beam:

$$\overset{\circ}{F} = -\overset{\circ}{V} \frac{4 Z^2 e^4 n_e L_P}{m} \frac{1}{\left(V^2 + \Delta_{e,eff}^2\right)^{3/2}}, \qquad \text{(A.1.23)}$$

where $\Delta_{e,eff}$ is the effective electron velocity spread with taking into account variations of the magnetic field line position in the transverse direction. The Coulomb logarithm is given by the expression:

$$L_P = \ln\left(\frac{\rho_{\max} + \rho_{\min} + \rho_{\perp}}{\rho_{\min} + \rho_{\perp}}\right). \qquad \text{(A.1.24)}$$

Where the minimum impact parameter is calculated in accordance with

$$\rho_{\min} = \frac{Ze^2}{m}\frac{1}{V^2 + \Delta_{e,eff}^2}. \qquad \text{(A.1.25)}$$

Maximum impact parameter in accordance with original formula is calculated as:

$$\rho_{\max} = \frac{v_i}{1/\tau_{flight} + \omega_p}, \qquad \text{(A.1.26)}$$

where τ_{flight} is the ion time of flight the cooling section (A.1.9), ω_p is the plasma frequency (A.1.4).

A.2. Model of the pellet target

To calculate expected number of the pellet crossing during given period of time for the ion circulating in a ring in the Betacool is used algorithm based on calculation of crossing probability as a function of the ion Courant-Snider invariants. The model of the pellet target was developed on the basic assumptions.

1. All the pellets have the same size, and the pellet shape can be approximated by box at dimensions l x x_p x y_p at uniform density, which is equal to the density of the frozen gas (l is the pellet size along the ion trajectory, x_p and y_p are the horizontal and vertical sizes). To keep the real density of the pellet the cube dimensions can be recalculated from the pellet diameter as $l = x_p = y_p = d\sqrt[3]{\pi/6}$, where d is the pellet diameter.

2. All the pellets move in vertical direction with the same velocity v_{pellet} and interval between them is equal to h.

4. The pellets form a flux at round shape of horizontal cross-section at radius r_f and the pellets are distributed uniformly inside it.

At long period of interaction the pellet target can be treated as a solid target at uniform density determined by the equation:

$$\rho_{eff} = \rho\frac{lx_p y_p}{\pi h r_f^2}, \qquad \text{(A.2.1)}$$

where ρ is the real pellet density, lx_py_p – the volume of the pellet, $h\pi r_f^2$ - the volume where the single pellet is located.

In the frame of discrete model of the target the program calculates the expectation of the number of the pellet crossings:

$$N_{cross} = P\frac{\Delta t}{T_{rev}} \ . \tag{A.2.2}$$

The probability P to cross the pellet during one revolution in the ring for given ion can be expressed as:

$$P = P_y P_x \tag{A.2.3}$$

where

$$P_y = \begin{cases} \dfrac{y_p}{h}, \ if \ \ y_p < h \\ 1, \ if \ \ y_p \geq h \end{cases} \tag{A.2.4}$$

is the probability to hit the pellet in vertical direction. The probability to hit the pellet in the horizontal direction P_x can be calculated as a ratio between the pellet flux cross-section and cross-section of the line along the ion trajectory at width of x_p (Fig.A.2.1).

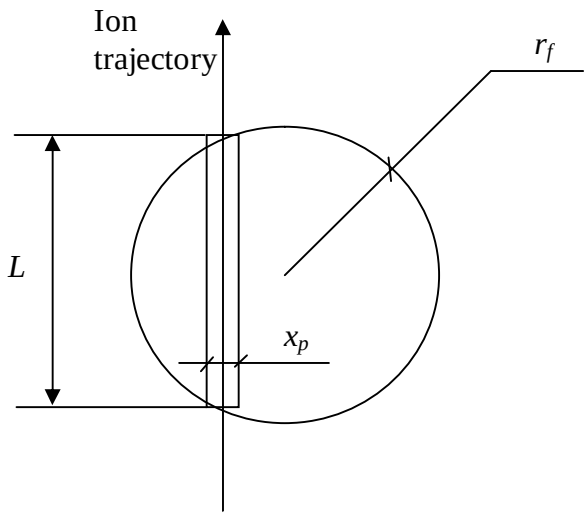

Fig.A.2.1. The pellet flux cross-section by the horizontal plane.

$$P_x = \frac{Lx_p}{\pi r_f^2}, \tag{A.2.5}$$

Length of such a line along ion beam orbit L does not depend on the ion vertical co-ordinate, and depends on horizontal ion co-ordinate x_i as follows:

$$L = 2\sqrt{r_f^2 - \left(x_i - \Delta_p\right)^2} \ , \tag{A.2.6}$$

when - $r_f < x_i < r_f$, and equal to zero, when the ion co-ordinate is bigger than flux dimensions. Here Δ_p is the horizontal displacement of the pellet flux centre from the ion equilibrium orbit.

During step of ion motion equation integration the ion oscillates in horizontal plane and the target length along the ion trajectory has to be averaged over the betatron oscillations. At given particle co-ordinates in the horizontal phase plane ($x_i, x_i^{/}$), its momentum deviation Δp/p and lattice parameters in the target position (alpha and beta function - α_x, β_x, horizontal dispersion – D and its derivative $D^{/}$) the particle horizontal co-ordinate in the target position can be expressed by the following formulae:

$$x_i(\varphi) = A_x \cos\varphi + D\frac{\Delta p}{p},$$
$$A_x = \sqrt{I_x \beta_x},$$

$$I_x = \beta_x x_\beta^{/2} + 2\alpha_x x_\beta x_\beta^{/} + \frac{1+\alpha_x^2}{\beta_x} x_\beta^2,$$
$$x_\beta = x_i - D\frac{\Delta p}{p},$$
$$x_\beta^{/} = x_i^{/} - D^{/}\frac{\Delta p}{p}. \qquad \text{(A.2.7)}$$

Here φ is the phase of the betatron oscillations. The mean target length $\langle L \rangle$ can be calculated as an integral:

$$\langle L \rangle = \frac{2}{\pi}\int_{\varphi_{min}}^{\varphi_{max}} \sqrt{r_f^2 - \left(x_i(\varphi) - \Delta_p\right)^2}\, d\varphi, \qquad \text{(A.2.8)}$$

where $\varphi_{min} = 0$ and $\varphi_{max} = \pi$, when the ion trajectory lies inside the pellet flux, or are calculated from elementary geometrical reasons:

$$\varphi_{min} = \arccos\left(\frac{\Delta_p + r_f - D\frac{\Delta p}{p}}{A_x}\right),$$
$$\varphi_{max} = \arccos\left(\frac{\Delta_p - r_f - D\frac{\Delta p}{p}}{A_x}\right). \qquad \text{(A.2.9)}$$

When the number of the pellet crossings during time Δt is known, calculating the number of crossings for all modeling particles one can calculate luminosity in accordance with:

$$L = \frac{N_i}{N_{MP}} \frac{\rho_{pellet}}{\Delta t} \sum N_{cross}, \qquad \text{(A.2.10)}$$

where N_i and N_{MP} are the total number of ions in the ring and number of modeling particles, ρ_{pellet} is the pellet thickness in atoms/cm^2.